A new Holocene relative sea-level curve for western Brittany (France): Insights on isostatic dynamics along the Atlantic coasts of north-western Europe

Goslin, J.; Van Vliet Lanoe, B.; Spada, Giorgio; Bradley, S.; Tarasov, L.; Neill, S.P.; Suanez, Serge

Quaternary Science Reviews

DOI:
10.1016/j.quascirev.2015.10.029

Published: 05/11/2015

Peer reviewed version

A new Holocene relative sea-level curve for western Brittany (France): insights on isostatic dynamics along the Atlantic coasts of north-western Europe

Jérôme Goslin [a*], Brigitte Van Vliet Lanoë [b], Giorgio Spada [c],
Sarah Bradley [d], Lev Tarasov [e], Simon Neill [f], Serge Suanez [a]

[a] *Geomer laboratory, UMR 6554 CNRS LETG, European Institute for Marine Studies, 1 place Nicolas Copernic, 29280 Plouzané, France*

[b] *Domaines Océaniques laboratory, UMR 6538 CNRS, European Institute for Marine Studies, 1 place Nicolas Copernic, 29280 Plouzané, France*

[c] *Dipartimento di Scienze di Base e Fondamenti, University of Urbino "Carlo Bo", Via Santa Chiara 27,I - 61029 Urbino (PU), Italy*

[d] *Institute for Marine and Atmospheric research Utrecht (IMAU); Utrecht University, Princetonplein 5, 3584 CC Utrecht, Netherlands*

[e] *Department of Physics and Physical Oceanography, Memorial University of Newfoundland, St. John's, NL A1C 5S7,Canada.*

[f] *School of Ocean Sciences, Bangor University,* Menai Bridge, Isle of Anglesey LL59 5AB, *United Kingdom*

* Corresponding author: Jérôme Goslin. jerome.goslin@univ-brest.fr. Tel.: +33 6 76 26 32 20

Abstract

This study presents new Relative Sea Level (RSL) data that were obtained in the Finistère region (Western tip of Brittany, France) and the implications those data have for the understanding of the isostatic dynamics at the scale of north-western Europe, and more specifically along the Atlantic and Channel coasts. New stratigraphic sequences were obtained and analyzed to derive 24 new Sea-level Index Points, in which 6 are basal. These new data considerably increase the knowledge we have of the RSL evolution along the coasts of Western Brittany since the last 8 kyr B.P. From this new dataset, RSL was estimated to rise continuously over the last 8 kyr with a major inflection at ca. 6 kyr cal. BP. Our results show large vertical discrepancies between the RSL records of Brittany and South-western UK, with the latter plotting several meters below the new data. From this comparison we suggest that the two regions underwent a very different pattern/amplitude of subsidence during the last 8 kyr which has implications for the spatial and temporal pattern of the peripheral bulge of the European ice sheets. We compared our data against predictions of Glacio-Isostatic Adjustment models (GIA models). There are large misfits between RSL observations and the predictions of the global (ICE-5G (VM2a) - Peltier *et al.*, 2004, GLAC1-b - Tarasov & Peltier, 2002; Tarasov *et al.*, 2012, Briggs *et al.*, 2014) and regional UK models ("BIIS" -Bradley, 2009; Bradley *et al.*, 2011-, model of "Kuchar"- Kuchar *et al*., 2012), which can't be resolved through significant changes to the deglaciation history and size of the British-Irish Ice sheet. Paleo-tidal modelling corrections indicate regional changes in the tidal ranges played a negligible role in the data-model misfits. Hence, we propose that the misfits are due to some combination of: (i) unaccounted mass-loss of far-field ice-sheets (Antarctic ice-Sheet or Laurentide Ice-Sheet) or, more likely, (ii) significant lateral variations in the Earth's structure across the English Channel.

Key words: Relative sea-level; Holocene; isostasy; GIA models; Tidal-range modeling; Earth structure; Brittany.

Introduction

During the last decades, there has been extensive effort to reconstruct Holocene relative sea-level (RSL) histories, with a clear revival of interest in more recent years, due to concerns relating to future global climate change. Reconstructions of past RSL have proved to be of prime interest to understanding present-day and possible near future sea-level variations (Bindoff *et al.*, 2007; Church and White, 2011; Church *et al.*, 2008; Engelhart *et al.*, 2009; Leorri *et al.*, 2012; Gehrels and Woodworth, 2013). This contributes to understanding the behaviour of coastal sedimentary systems during periods of RSL rise and provides improved constraints of the vertical movements of the solid Earth which have taken place since the Late Glacial Maximum (LGM). During the Holocene, the main processes driving regional RSL changes are (i) eustatic sea-level rise (ESL) (i.e. the increase of the volume of the oceans induced by the retreat of the continental ice-sheets, regional glaciers and steric changes), (ii) isostatic dynamics (commonly referred to as GIA ; Glacio-Isostatic Adjustments), i.e. changes in the topography of the solid Earth induced by the decrease of the ice load following the retreat of the major land based ice-sheets ("glacio-isostasy") and from the increase of the water-loading of the continental shelves ("hydro-isostasy") and (iii) tectonic movements, the relative importance of all these parameters in RSL evolution being variable during the Holocene. At mid- to high-latitudes, the northern hemisphere was covered by large land-based ice-sheets (e.g. Laurentide, British-Irish and Fennoscandian Ice-Sheets, noted LIS, BIIS and FIS, respectively, but also the Innuitian, Cordilleran, Greenland and Kara-Barents ice-sheets) and as such glacio-isostatic dynamics have been the predominant processes in RSL evolution since the middle Holocene.

Glacio-Isostatic Adjustment (GIA) resulting from the melting of these northern hemisphere ice-sheets is still ongoing, and will play a major role in present-day and near-future RSL changes along the coasts of the northern hemisphere. The Holocene RSL signal across NW Europe is mainly driven by the GIA resulting from the regional ice sheets (i.e. the "Fennoscandian Ice-Sheet" and the "British Irish Ice-sheet", respectively noted FIS and BIIS hereafter). Therefore, recent sea-level observations from tide gauges and satellites contain remnant GIA signals that must be taken into account when isolating eustatic and steric signals (e.g. Peltier, 2001; Tamisiea and Mitrovica, 2011, Wöppelmann & Marcos, 2012). Understanding the regional GIA dynamics is hence crucial before reliable scenarios of future regional RSL rise can be proposed. To address this problem, numerical geophysical models (termed Glacio-Isostatic Adjustment models or "GIA models") have been developed since the early seventies. These models provide RSL predictions for any particular location on the surface of the Earth by solving a unified set of equations (the Sea-Level Equation, "SLE", Farrell and Clark, 1976) that merges (i) an "Ice model", which defines the history of the major land-based ice sheets and (ii) a rheological model ("Earth model") describing the behaviour of the Earth's surface in response to surface load changes, and (iii) the changes in gravitational field induced by the redistribution of the mass at the Earth's surface (melting of the ice-sheets) and within the Earth's interior (displacement of mantle material due to isostatic adjustment) (e.g. Mitrovica and Peltier, 1991; Peltier, 1998; Mitrovica and Milne, 2003; Spada *et al.*, 2012). Significant regional misfits continue to exist between predicted and observed RSL (e.g. Engelhart *et al.*, 2012; Ostanciaux *et al.*, 2012), which suggest errors and/or simplifications in the ice history and/or earth rheology components of the GIA models. Hence, precise and reliable RSL observations are still needed in many places to better constraint GIA models.

In Northwestern Europe, sea-level reconstructions have been produced since the seventies. The most intensive research efforts were conducted around the British Isles, especially along the northern and eastern coasts of the UK. The dense RSL dataset obtained in Great Britain served as a basis for the development and the fine-tuning of regional GIA models (Shennan *et al.*, 2006; Bradley *et al.*, 2011; Kuchar *et al.*, 2012). Results recently published by Bradley *et al.* (2011) and by Shennan *et al.*

(2012) agree for present-day land subsidence rates of ca. 0.5 to 0.8 mm/yr^{-1} in Devon and Cornwall. However, Bradley *et al.* (2011) and Kuchar *et al.* (2012) note misfits of several meters between geological reconstructions and regional model predictions for the Southwest UK. In this study, we propose to push the comparison between Holocene RSL and GIA model predictions a few hundred kilometers south on the other side of the English Channel.

Within the framework of a coastal risk assessment research program (ANR COCORISCO, French National Research Agency), extensive fieldwork has been conducted during the past four years around the Finistère peninsula (Western Brittany, France). Along with the study of Holocene paleo-storminess, which was the prime objective of the research program (Van Vliet *et al.*, 2014a, 2014b), many of the sampled sedimentary sequences could also be successfully analyzed to derive RSL data.

The first objective of this study is to obtain new precise and reliable sea-level index points (SLIPs) for the Western Brittany region with a particular emphasis placed on recovering compaction-free basal SLIPs. The second objective is to explore the implications of these new RSL data for the isostatic dynamics of the coasts of Western Europe, following a two-step approach. First, we perform a regional comparison of our data with the RSL history proposed for the closest region for which a well-constrained Holocene RSL record is available (Southwest UK). We thereby evaluate if isostatic gradients can be identified on the basis of RSL data alone. Second, we compare our new data against predicted RSL from both global and regional published GIA models. We also discuss the origin of the misfits between our data and model predictions, with a particular emphasis on local- to regional-scale factors which can potentially influence paleo-RSL.

1. Relative sea-level histories of the French Atlantic and Channel coasts: previous studies

Despite the several RSL studies that have been conducted since the seventies along the French Channel and Atlantic coasts (Delibrias and Guillier, 1971; Ters, 1973; Morzadec-Kerfourn, 1974; Ters, 1986, Van de Plassche, 1991; Goslin *et al.*, 2013; Stéphan *et al.*, 2014), there remains a lack of reliable and high-quality Holocene basal SLIPs (Stéphan and Goslin, 2014). For the Finistère region (western tip of Brittany), only two studies achieved a sufficient data density to derive Holocene RSL reconstructions (Morzadec-Kerfourn, 1974; Stéphan *et al.*, 2014). However, none of these studies included data prior to 6000 yr B.P., nor sufficient basal data to provide reliable conclusions on the Holocene RSL evolution in Western Brittany. Additionally, Goslin *et al.* (2013) showed that a reassessment of the oldest data from the region, extracted by state-of-the-art methods, leads to a further reduction by up to two thirds of the number of SLIPs which can be considered reliable. At a larger scale, the data from Delibrias and Guillier (1971), Ters (1973, 1986), Morzadec-Kerfourn (1974) and Van de Plassche (1991) formed the main constraint for modeling work of Lambeck (1997) and Leorri *et al.* (2012). These studies aimed to quantify the contributions of the glacio- and hydro-isostatic components in the RSL histories of the Atlantic coasts of Europe. Both studies proposed that a North-South trending glacio-isostatic gradient could have influenced the European Atlantic coasts, due to the influence of the north-western European peripheral bulge that formed in response to the combined influence of the BIIS and FIS ice loads. This gradient would have extended from the southern coasts of UK to the south of the Bay of Biscay (Lambeck, 1997) or even as far as South Portugal (Leorri *et al.*, 2012). However, as Goslin e*t al.* (2013) recently suggested, the field-data used by Lambeck (1997) and by Leorri *et al.* (2012) for the Brittany region should not be considered reliable enough to conclusively validate the outputs of their GIA models. Hence, the proposed isostatic gradients along the western Atlantic coasts of France and Spain are still to be ascertained. In northwest Europe, Vink *et al.* (2007) evidenced for a continuous heightening of the RSL records when progressing from northern France to southern Denmark that illustrated a progressive damping of the FIS peripheral bulge isostatic subsidence towards its tail. Unfortunately, the lack of basal data along both sides of the English Channel coasts has up to now prevented from following this trend further west, while the signal becomes more and more complex as it sums up with the isostatic signal induced by the BIIS loading and hydro-isostasy. Finally, offsets between tide-gauge records at Brest and Newlyn (Cornwall, Southwestern UK) (ca. 1.41 mm/year and 1.74 mm/year, respectively) hint for different recent RSL rise rates between the two locations (Woodworth *et al.*, 1987; Douglas, 2001, Haigh *et al.*, 2009). Considering the proximity of the two stations, located ca. 200 km apart, and the absence of any tectonic active process which could account for such a ca. 0.3mm.yr^{-1} differential in vertical land-movement, this difference is still unexplained (Douglas, 2008; Wöppelmann *et al.*, 2008, Haigh *et al.*, 2009).

In this context, obtaining new high-quality RSL data in the Finistère (Western Brittany) region was critical to improving the understanding of Holocene isostatic dynamics and the RSL history along the Atlantic coasts of Europe. Located ca. 200 kilometers directly south of Cornwall, Brittany also remained ice-free during the Late Pleistocene. It can be considered, together with Southwest UK

(Massey *et al.*, 2008), as a key area to constrain the extent, amplitude and dynamics of the north-western European peripheral bulge and the ESL signal over this period.

2. Regional settings and study sites

2.1 Geological, geodynamic and physiographic settings

The Finistère region is situated at the western end of the Armorican massif, which is bounded on this northern termination by the North-Armorican scarp marking the entrance of the English Channel geological system. The latter is characterized by a system of grabens, delimited by a dense network of multi-kilometric deep crustal faults (up to 7 to 10 kilometers, Evans, 1990; Lericolais, 1997; Lagarde *et al.*, 2003). The northern and southern parts of the Finistère region are composed of granitic batholiths domains that were emplaced during the Cadomian and Variscan orogenies. In those regions, the basement is mainly composed of endogenous granites and metamorphic rocks (gneisses and amphibolites). In between those plutons, a synclinal deformation hosts sandstones and shale formations of Palaeozoic age. Brittany is considered to have undergone a long step-wise passive margin subsidence since the opening of the Bay of Biscay between the Jurassic and the Late and Early Cretaceous (Evans, 1990; Van Vliet *et al.*, 1997; Bonnet *et al.*, 2000). The Finistère region is currently undergoing compression due to the ongoing northward motion of the Iberian plate (Wyns, 1991; Bonnet *et al.*, 2000). This dynamic results into a low-intensity and diffuse seismicity that remains concentrated along two majors faults (the *North-* and *South-Armorican Shear Zones,* Lagarde *et al., 2003*). Large earthquakes (of magnitudes equal to or greater than 5.5) are unusual (centennal) and mainly concentrated within the Cotentin region, in the central part of the English Channel. Seismic activity can be considered to have been of equal magnitude and frequency during the Holocene, and thus to have had none or insensible impacts on the sedimentary sequences of this period.

2.2 Rationale for study sites selection

The Finistère peninsula is exposed to macro- to meso-tidal conditions, with spring tidal ranges decreasing from up to 7.5 m in the north to ca. 4 m in the south of our study area (table 1). Present-day local tide data were obtained either from the nearest tide station(s) (SHOM, 2012, French Navy Oceanographic Agency) or by interpolation between the two nearest tide stations.

New stratigraphic data were collected from six sites (Guissény, Landéda, Porsmilin, Treffiagat, Kermor-Tudy and Guidel) which covered the entire study area (Fig.1), and sampled a range of very diverse morphological configurations: open embayments, inner rias, open coast and estuarine back-barrier sites (classification after Allen, 2000). The spatial spread of the study sites was chosen to improve the regional representation of the reconstructed RSLs. Finally, the extended north-south spread of the study sites allowed (i) the differences in tidal ranges to be assessed and (ii) investigation of the RSL signal from sites located at variable distances from the former centres of the paleo-ice-sheets (and thus situated in different positions along the glacio-isostatic gradient).

3. Material and Methods

3.1 New data

3.1.1 Sampling and surveying

Most of the sampling was from coring (using an Eijkelkamp 60-mm diam., hand-held motor-driven percussion corer that extracts 1m sections in plastic tubes). For some sequences that comprised thick layers of sand and a thick water table (Kermor and Guidel sites, see fig.1 and section 4.1), buoyancy problems prevent us from using percussion corers. The BRGM's (French Research Agency for Geology and Mines) sedidrill mounted-rig was then used. Extreme precautions were taken to identify and sample undisturbed sediment and drillings were cross-checked in order to ensure the stratigraphic continuity. This latter is also ensured by the high-resolution paleo-environmental studies that have been made on the same sequences (Fernane *et al.*, 2014, 2015). Finally, some short sequences were retrieved from the foreshore using a hand-gouge prior to this study. All sites were positioned using a Trimble 5800 DGPS and tied to IGN (French National Geographic Institute) benchmarks. Elevations were determined with respect to the NGF datum (French levelling datum).

3.1.2 Sedimentary analyses and dating

All sedimentary sequences were described in the laboratory in terms of grain size, colour, organic and macrofossil contents. Particular attention was paid to identify possible reworked levels or erosional surfaces. Radiocarbon AMS dating was performed after the material was washed, dried and carefully selected under the microscope. Whenever possible, plant remains were preferred as their fragility reduces the risk of re-deposition (Gehrels *et al.*, 1996; Törnqvist *et al.*, 1998; Gehrels, 1999).

Potentially reworked material such as drift wood or charcoal was dated only when no other material was sufficiently available. Marine shells were dated only if found complete and in living position within the deposits. AMS radiocarbon measurements were performed at the "*Laboratoire de Mesure du Carbone 14*" (Gif-S/Yvette) and at the Poznan Radiocarbon Laboratory (Poland). Dates were calibrated after correction for isotopic fractionation using Calib 7.0 with the IntCal13 and the Marine13 calibration curves for the terrestrial and marine material, respectively (Reimer *et al.*, 2013). Dates are reported with a 2σ (95%) confidence interval.

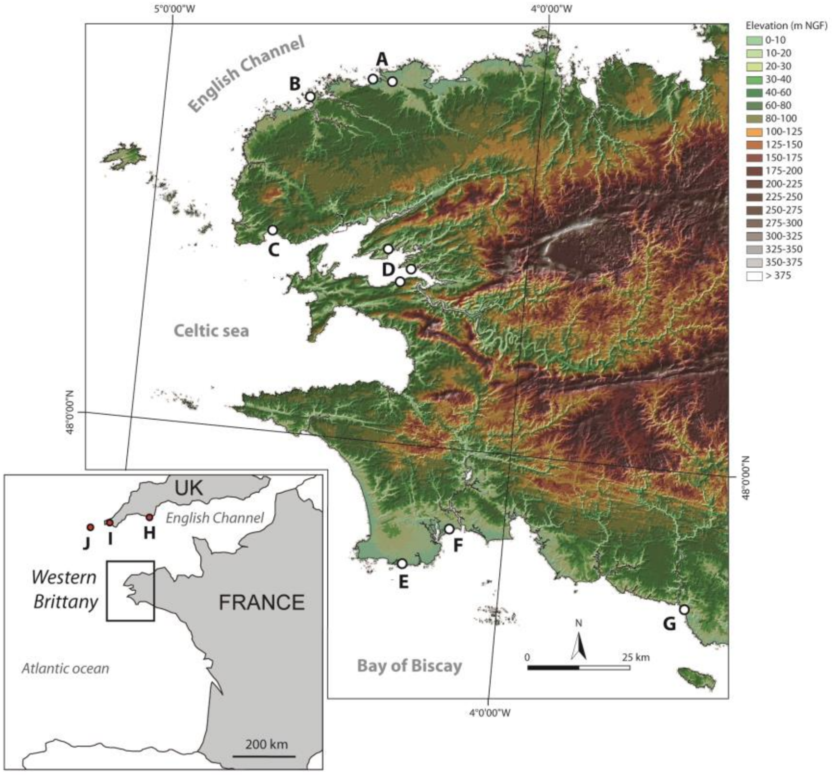

Figure 1 - Location map of the study area and of the study sites. A) Guissény -Tresseny (inner dot) & Guisseny-Vougot (outer dot), B) Landéda, C) Porsmilin, D) Bay of Brest, E) Treffiagat, F) Kermor-Tudy, G) Guidel Loc'h. (H, I, J) are the locations of the SW England Holocene RSL records to which we compare our data to (section 4.4).

3.1.3 Paleo-RSL elevation reconstruction

We follow the SLIP methodology (Shennan, 1986; Van de Plassche, 1986) to reconstruct RSL changes. For a general view on RSL reconstruction methods and on the SLIP methodology, readers are referred to Shennan *et al.* (2015). In short, a valid index point requires the following information: (i) the latitude and longitude of the site, (ii) the altitude (and associated uncertainties) of the surface, (iii) an age and (iv) an Indicative Meaning (IM). The IM of a sample is the altitude of the original deposition tied to a paleo-tidal reference level (e.g. Mean High Water Spring Tide MHWST or Mean tide Level MTL). In this study, the elevation of each SLIP was calculated according to the following formula:

$$SLIP = H - D - I + T + A$$

where *H* is the elevation of the top of the core in meters relative to the reference water level; *D*, the depth of the sample in the core in meters; *I*, the Indicative Meaning in meters (in this study the IM was taken relative to the Mean High Water Spring Tide of each site), T the correction brought to I to include changes in paleo-tidal ranges and A the potential post depositional autocompaction undergone by the studied intercalated layer since deposition (uncorrected within this study).

SLIPs are then weighted with *Es* the sum of altitudinal error terms potentially introduced at each stage of the reconstruction. For each index-point, *Es* can be calculated from the following expression (Horton *et al.*, 2000):

$$E_s = \sqrt{E_1^2 + E_2^2 + E_n^2}$$

where $E_1 \ldots E_n$ are the elevation uncertainties affecting the given sample. For example (i) the possible deformation of the sequences during the coring (*e.g.*, compaction induced by the percussion); (ii) the non-verticality of the core that can lead to an under-estimation of the sample depth; (iii) the potential flexure of the rods during hand-augurings; (iv) the potential “twirl” effect on the intercalated samples retrieved with the screw-drilling rig; (v) the leveling uncertainties inherent to DGPS measurements; (vi) the error in tying the station altitude to the IGN benchmark, and finally (vii) the uncertainty inherent to the calculation of the IM, which is defined as the “Indicative Range” (IR). This later uncertainty depends on the methodology used to determine the Indicative Meaning and on the specific tidal parameters of each site. The various terms used to calculate the elevation uncertainties are summarized in table 2.

Changes in tidal regimes during the Holocene are an additional, and significant, source of error in RSL reconstructions. Indeed, paleo RSL positions are most often derived from indicators which were emplaced within the high-tide domains. Therefore, changes in the tidal ranges through time can result in paleo-RSL positions that differ from the "true" Mean Sea Level (MSL) signal that represents "allogenic" RSL change (as termed by Gehrels, 1995). Estimating the paleo changes in local tidal ranges is even more crucial when observational data are to be compared with RSL predictions produced by GIA models, which are defined relative to the MSL. In this study, the effects on RSL reconstructions of possible changes in the tidal range in our study area have been obtained following a modelling approach, described in section 3.3.2. This is one of the few studies to date where paleo-tidal corrections have been applied in the reconstruction of RSL histories in NW Europe (Shennan *et al.*, 2000; Shennan and Horton, 2002, Neill *et al.*, 2010).

Indicative meanings are traditionally determined through the use of micro-fauna assemblages (e.g. Horton *et al.*, 2006; Massey *et al*., 2008; Kemp *et al.*, 2009, Kemp *et al.*, 2013, Stéphan *et al.*, 2014). Within most of our sedimentary sequences, foraminifera were scarce or totally absent while diatoms were rare and limited to some particular layers. To overcome this difficulty, we determined indicative meanings using salt-marsh surface sediment stable carbon isotope ratios ($\delta^{13}C$) and bulk geochemistry (TOC, TN, C/N ratio). The latter is an alternative RSL reconstruction approach whose usability in micro-fauna poor saltmarsh environments has been recently highlighted (Engelhart *et al.*, 2013; Goslin, 2014). We used the modern geochemical reference constructed for our study region by Goslin (2014). Complete details on the development and use of this reference, along with the protocols followed and the obtained results can be found in Supplementary Online Material (SOM, appendix S1). In short, $\delta^{13}C$, TOC and TN measurements were made on modern sediments sampled at the surface of three saltmarshes located in Brittany. Samples were taken along transects running from the low marsh to the high-marsh brackish to freshwater transitional domain. We combined the results obtained from the surfaces of the three marshes to build a modern geochemical regional training set. Clustering statistical analyses (Partitionning Around Medoids, PAM) were then made on the whole dataset to decipher whether groups of comparable $\delta^{13}C$, TOC and TN values could be identified along the tidal frame. This way, we identified four elevational groups characterized by specific values of $\delta^{13}C$, TOC and TN and altitudinally bounded. Palaeo salt marsh elevations (and *i.e.* palaeo RSL positions) were then reconstructed from Holocene cores using Linear Discriminant Functions, that allow to determine the probability for palaeo observations (core samples) to be allocated to one of pre-specified classes (here, to one of the biozones obtained above by PAM from modern samples and characterized by specific values of $\delta^{13}C$, TOC, and TN). Palynological data were also used when available (Morzadec-Kerfourn, 1974; Fernane *et al.*, 2014). Deposits that could not be directly related to the reference water level were used to provide limiting points: terrestrial freshwater deposits gave high-limiting points; and marine deposits, low-limiting points (Shennan *et al.*, 2015). Indicative meanings that were used are summarized in table 3.

As proposed by Engelhart *et al.*, (2012), we classified our SLIPs into three categories (see Engelhart *et al.*, 2012 for a full description of these categories): (1) Base of Basal deposits (noted "BB"), considered to provide compaction-free index-points (thus of prime reliability for RSL reconstruction); (2) Basal deposits (noted "B", possible but limited autocompaction); finally (3) the SLIPs derived from Intercalated deposits (noted "I", prone to autocompaction, non-corrected within this study).

3.2 Additional data

RSL data previously produced by Morzadec-Kerfourn (1974) in the North Finistère region were thoroughly re-assessed (recalibration of the dates, new determination of the indicative meaning, assignation of error terms) before they were incorporated into our dataset. The details of these re-assessments can be found in Goslin *et al.* (2013). This included reassessment of the salinity regime of some of the basal peat from these previous studies using a mixed palynological and geochemical approach (Goslin *et al.*, 2013). When it could be ascertained that these basal peats were deposited within a brackish environment, it was considered that they formed between the Mean High Water Neap Tide (MHWNT) and the Highest Astronomical Tide (HAT) levels (Goslin *et al.*, 2013). Recent RSL data published by Stéphan *et al.* (2014), mostly obtained from salt-marshes of the Bay of Brest, were incorporated as published. Data we retained from previously published studies of Goslin *et al.* (2013) and Stéphan *et al.* (2014) are summarized in table 5, with their original error terms.

3.3 Modelling

3.3.1 Geophysical glacio-isostatic adjustment modelling

We compared the RSL predictions of five GIA models (five different ice and Earth models combinations) against the new RSL data obtained in this study. We utilised two global ice models. The "ICE-5G" model, developed by Peltier (2004) is a non-glaciological ice-loading model that has been hand-tuned to provide best-fit predictions to an extensive global database of RSL and GPS records.

The second global (“Glac1-b”) model is a set of interim results for an ongoing large ensemble Bayesian calibration of the Glacial Systems Model (GSM) which includes a 3D thermomechanically coupled ice sheet component (Tarasov *et al.*, 2012; Tarasov, 2013). The constraint data set for the calibration includes most of the same data use to tune ICE-5G along with additional ice sheet specific data such as strandline records of pro-glacial lake levels and marine limits for North America and the dynamic model fit to present-day observed ice topography and thickness for Antarctica and Greenland. Glac1-b contains components from Tarasov & Peltier, 2002 (Greenland); Tarasov *et al.*, 2012 (North America), Briggs *et al.*, 2014 (Antarctica), and a yet unpublished component for Europe (that has been validated for the Barents/Kara region against GRACE observations in Root *et al.*, 2015). We also utilized two regional models which were combined with the global ice model “Brad15”, an extension of the global model of Bassett *et al.* (2005) constrained with new Holocene RSL data from China and Malay-Thaïland (Bradley, 2009; Bradley, 2011; Bradley *et al.*, submit.). The “BIIS” model was originally published in Bradley *et al.*, (2011). It was developed by combining Brad15 with a UK-Ireland ice sheet model (Brooks *et al.*, 2008). The latter was developed to fit the UK geomorphological data and fine-tuned to fit the British-Irish RSL database and GPS data (Bradley *et al.*, 2009, Bradley, 2011). The second regional (“Kuchar”) model (Kuchar *et al.,* 2012) was derived from output of a glaciological three-dimensional thermomechanical ice sheet model for the BIIS (Hubbard *et al.*, 2009).The ICE-5G and GLAC1-b models respectively use the VM2a and VM5a Earth-models for the European region. These Earth-models were tuned to provide the best-fit solution to near-field Hudson Bay and Angerman River (Sweden) RSL records (Peltier, 2004). Conversely, we ran the “BIIS” and the “Kuchar” models with Earth-models whose parameters were fine-tuned against near- and intermediate-field RSL data from the British Isles and present-day GPS land vertical motion data (Bradley, 2011; Bradley *et al.*, 2011). All these GIA models are based on the self-consistent SLE theory first introduced by Farrell and Clark (1976). The ICE-5G (VM2a) model of Peltier (2004) was originally developed with a lithosphere thickness of 90 km. We ran it with upper mantle viscosities of 0.5×10^{21} Pa.s, and lower-mantle viscosities of 2.7×10^{21} Pa.s. GLAC1-b uses Peltier's VM5a Earth model. VM5a is a variant of VM2a, with lithospheric thickness reduced to 60 km and an additional 40 km thick low viscosity layer directly below the lithosphere (1.0×10^{21} Pa.s). It has upper mantle viscosities of 0.5×10^{21} Pa.s and lower-mantle viscosities of 1.6×10^{21} Pa.s (upper 500 kms) and 3.2×10^{21} Pa.s (rest of lower mantle). “BIIS” (Bradley, 2009, Bradley *et al.*,2011, Bradley *et al.*, *submit.*)

and Kuchar *et al.'s* (2012) regional models adopt a lithosphere thickness of 71 km, upper- and lower-mantle viscosities of 0.5×10^{20} Pa.s and 3×10^{22} Pa.s for the former and of 0.3×10^{20} Pa.s and 2×10^{22} Pa.s for the latter, respectively.

3.3.2 Paleo-tidal modelling

We computed changes in tidal ranges for our study sites using the 3D tidal model of Neill *et al.* (2010). The reader is referred to Neil *et al.* (2010) for greater details about model parameters and calculations. In summary, the evolution of the principal semi-diurnal (M_2) and solar (S_2) tidal constituents were simulated to describe “mean” spring and neap ranges and interpolated initially by running the outer coarser global tidal model of Uehara *et al.* (2006), modified to account for the updated ICE-5G (VM2a) GIA model (Neill *et al.*, 2010). A $1/24^{th}$ degree resolution grid was used for the tidal range computations (Neill *et al.*, 2010). Due to negligible differences at the scale of the shelf after 6ky B.P., we did not performed calculations after this date (Neill *et al.*, 2010). Thus, we obtained tidal ranges for 5 kyr, 4 kyr, 3 kyr, 2 kyr and 1 kyr B.P by linear interpolation between model output values. We corrected and recalculated the Indicative Meanings and the Indicative Ranges of our modern regional tidal zones to account for the tidal conditions that prevailed at each site at the time of deposition of the various sedimentary layers. The output figures of the model runs are provided as supplementary information in SOM (appendix S2), for each study site.

4. Results and discussion

4.1 Stratigraphies

Complete information regarding the data presented below (e.g. datings, depth, geochemical measurements, IM, IR) is summarized in table 4.

Kerlouan – Guissény (A. North Finistère)

Tressény marsh

Core GUIS-C2 was retrieved from the central part of the inner cove salt-marsh of Tressény (fig. 2-1). The sequence sampled by the GUIS-C2 core consists in 0.4 m of Pleistocene material, progressively topped with ~0.6 m of a highly organic stratified silty peat, containing rare foraminifera and *Phragmites australis* macroremains (fig.2-3), indicating its brackish character. The base of the basal peat layer yielded geochemical values characteristic of high-marsh deposits (index n° 17, table

4). This basal deposit evolves into a 0.15 m thick black-peat layer that denotes the onset of slightly regressive conditions towards highest marsh deposit environments on the site around 5.1 kyr B.P. and 4.7 kyr B.P.

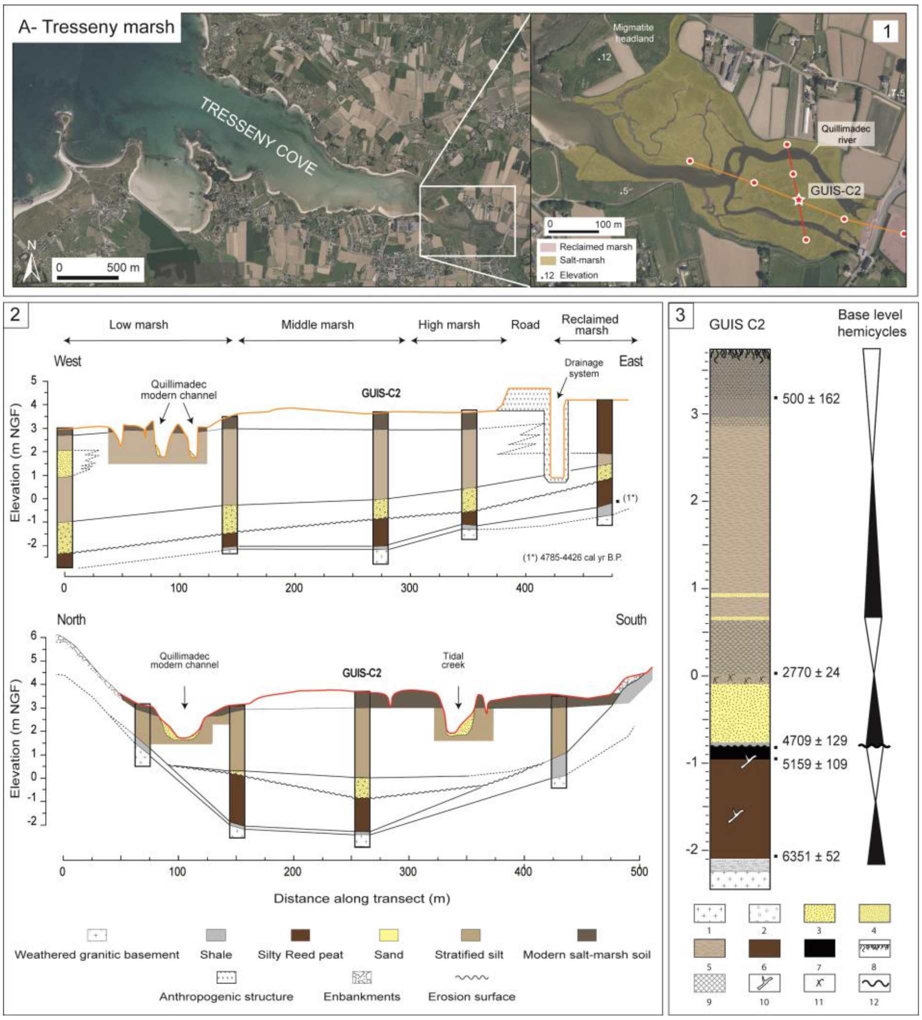

Figure 2 - 1) Map of the Tresśeny marsh (noted A on Fig.1) showing the location of the coring transects**.** The red star locates the GUIS-C2 sampled core. 2) Detailed stratigraphy from coring transects taken through the marsh (adapted from Stéphan *et al.*, 2014), (1*) is an informative dating taken from Stéphan *et al.* (2014) and unused in this study. 3) Complete stratigraphic log of the GUIS-C2 core.1- Weathered granite basement, 2- Angular gravels and pebbles, 3- Coarse sand, 4- Fine sand, 5- Laminated silt dominated minerogenic deposit, 6- Silty Reed peat, 7- Black peat, 8- Humic soil horizon, 10- wood fragments, 11- fragmented shells, 12- Erosion surface.

Commentaire [BVVL1]: NEW FIGURE ADDED

The black peat layer is abruptly eroded at its top. A 0.6 m thick sand layer rests above the peat layer, showing high energy granulometric characteristics and evolving upward from terrestrial material at its base towards coarser shell-rich marine sand. The top of the sequence is composed of alternating layers of organic silty layers and some sand enriched layers, progressively increasing in organic content before reaching the contemporaneous salt-marsh soil (3.75 m NGF, Fig. 2). The silty layers in the top of the sequence show evidence of deposition within a channel environment and contain signs of allochtonous material embedded in the sediment (in particular, very low $\delta^{13}C$ and C/N values). Therefore these layers were not considered reliable for RSL reconstruction. The roof of the infill, dated ca. 500 yr B.P., displays all the geochemical characteristics of middle to high marsh environment (index n°1, table 3).

Vougot Beach

The sequence preserved at the bottom of the Vougot beach at Guisseny was investigated by one hand-auguring (see sequence Guis-S2, Fig.3). Within the Guis-S2 sequence, 0.65 m of brown peat was retrieved before reaching the underlying loess formation. The base of the basal peat layer (-1.15 m NGF) shows signs of brackish environment deposition (embedded reed fragments).

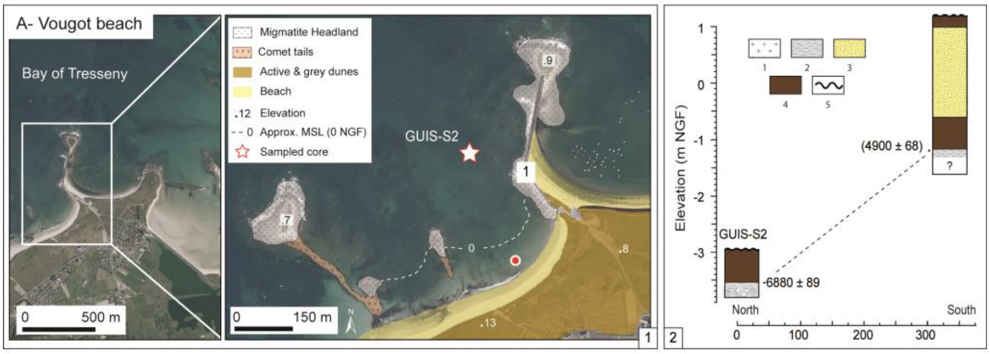

Figure 3 - 1) Map of the Vougot beach (noted A on Fig.1) showing the location of the cores**.** The red star locates the GUIS-S2 sampled core. 2) Detailed stratigraphy from coring transects taken through the marsh. Dating in brackets is given for informative purposes and in not used in this study. 1- Weathered granite basement, 2- Silt, 3- Medium sand, 4- Reed peat, 5- Erosion surface.

Commentaire [BVVL2]: NEW FIGURE ADDED

Landéda – Tariec (B. North Finistère)

In core ‘TAR-S1’, an approximately 0.6 m-thick highly fibrous peat was reached at -3 m NGF (Fig.4), It is principally composed of embedded reed-leaves fragments and directly overlaid the Pleistocene loessy silt level. It is topped by a ca.1 m-thick sand layer. The blended *Phragmites australis* and *Juncus maritimus* macro-remains suggest a brackish highest high marsh environment.

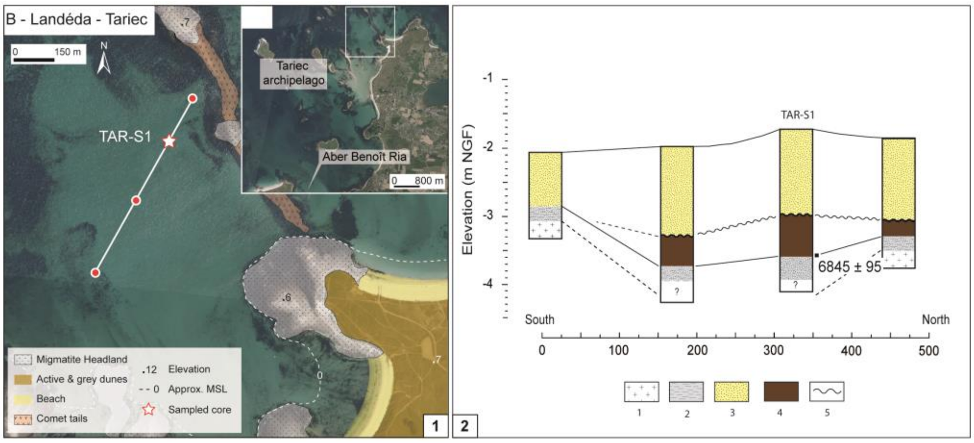

Figure 4 - 1) Map of the Tariec foreshore (noted B on Fig.1) showing the location of the coring transect**.** The red star locates the TAR-S1 sampled core. 2) Detailed stratigraphy from the coring transect taken through the site. 1- Granite basement, 2- Silt, 3- Medium sand, 4- Reed peat, 5- Erosion surface.

Commentaire [BVVL3]: NEW FIGURE ADDED

Porsmilin (C. West Finistère)

Five piston cores were retrieved from the foreshore to the bottom of the back-barrier swamp (Fig. 5). Only core PorsC1, which was retrieved at the bottom of the beach, could successfully be interpreted for RSL reconstruction purposes as the cores retrieved from the inner areas of the marsh only contained freshwater deposits that delivered non informative limiting points (Fig.5). In PorsC1, the roof of the weathered basement was reached at -5 m NGF. Over this basement lays ca. 0.3 m of gravel–rich clay, topped with around 2 m of slightly clayey sand of probable channel origin. Above this layer, the upper half of the sequence is characterised by a shift towards organic and stratified silt deposits, intercalated with woody peat layers (Fig.2). The base of the basal peat (-3.3 m NGF) was dated at 7 ky cal. B.P. A high marsh depositional environment can be inferred from the geochemical values obtained on this deposit. This is in accordance with the palynological assemblages described by Fernane *et al.* (*2014*) that show dominating *Poacea* and *Cyperacea* pollen spores (which can correspond to plant species adapted to a brackish environment, such as *Spartina altinerflora*, *Phragmitus australis* and *Juncus roemarianus*). The upper half of the sequence shows constant signs of pyritisation embedded in the sedimentary mat

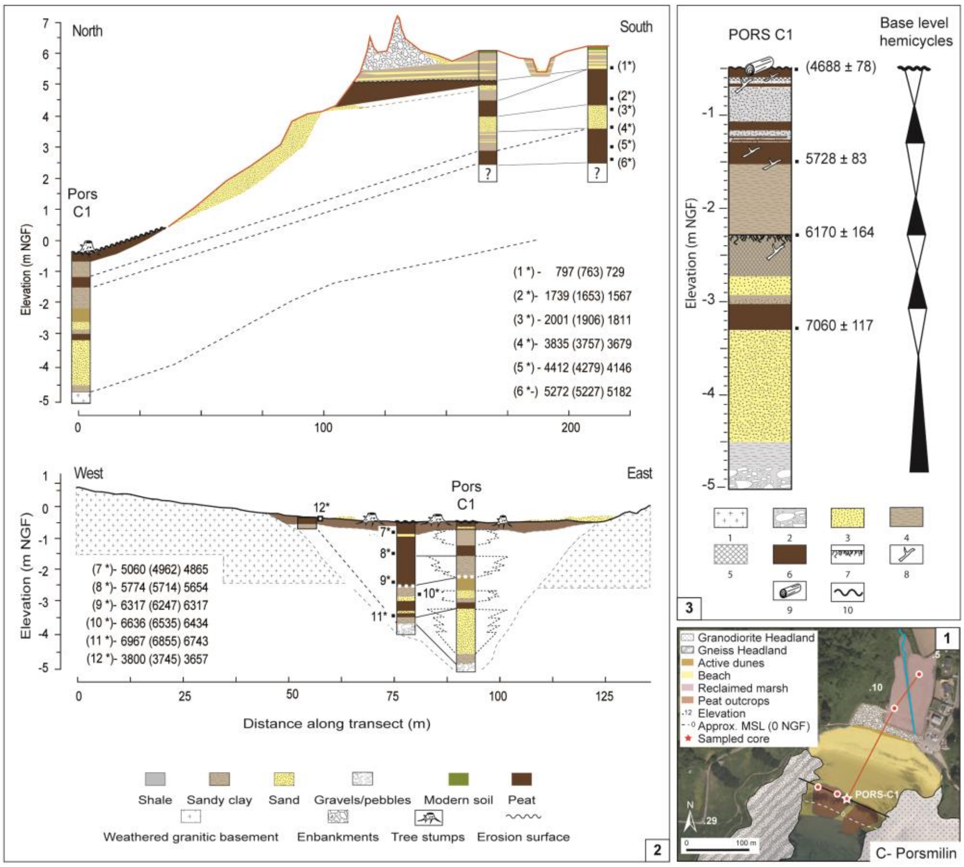

Figure 4 - 1) Map of the Porsmilin site (noted C on Fig.1) showing the location of the coring transects and of the sampled core**.** The red star locates the PORS-C1 sampled core. 2) Detailed stratigraphy from coring transects taken through the marsh and the foreshore. Datings in brackets (Fernane *et al.*, 2014) are given for informative purposes and are not used in this study. 3) Complete stratigraphic log of the PORS-C1 core:1- Weathered granite basement, 2- Angular gravels and pebbles, 3- Sand, 4- Stratified silt deposit, 5- Highly organic layer, 6- Peat, 7- Humic soil horizon, 8- wood fragments, 9- Tree stump, 10- Erosion surface.

Commentaire [BVVL4]: NEW FIGURE ADDED

Treffiagat (D. South Finistère)

Two cores were taken near the swamp in the back-barrier zone, respectively at 2.2 m NGF and 1.75 m NGF, that were merged to build a compound complete sequence (Fig.6). The observed sequence begins at -1.25 m NGF with a ~0.3-m thick Pleistocene silty-mud complex (traces of oxidation and several roots remains attest of its aerial exposure) overlaying the weathered basement. Over this first layer, a 30-cm thick organic silty peat layer is found, progressively turning into a wood-rich black peat above *ca*. -0.75 m NGF (Fig.6). This peat layer is capped by ~1.70 m medium to coarse sand layer, of sand-barrier origin, whose onset was dated ca 1000 cal. B.P. Micromorphological analyses revealed an extensive presence of pyrite within the matrix of the basal Holocene silty peat layer, along with *Chrysophyceae* fragments (unspecified species). Geochemical data from this basal deposit imply deposition in a mid- to low marsh environment. In contrast, no direct evidence for brackish influences could be obtained from the overlying peat deposit.

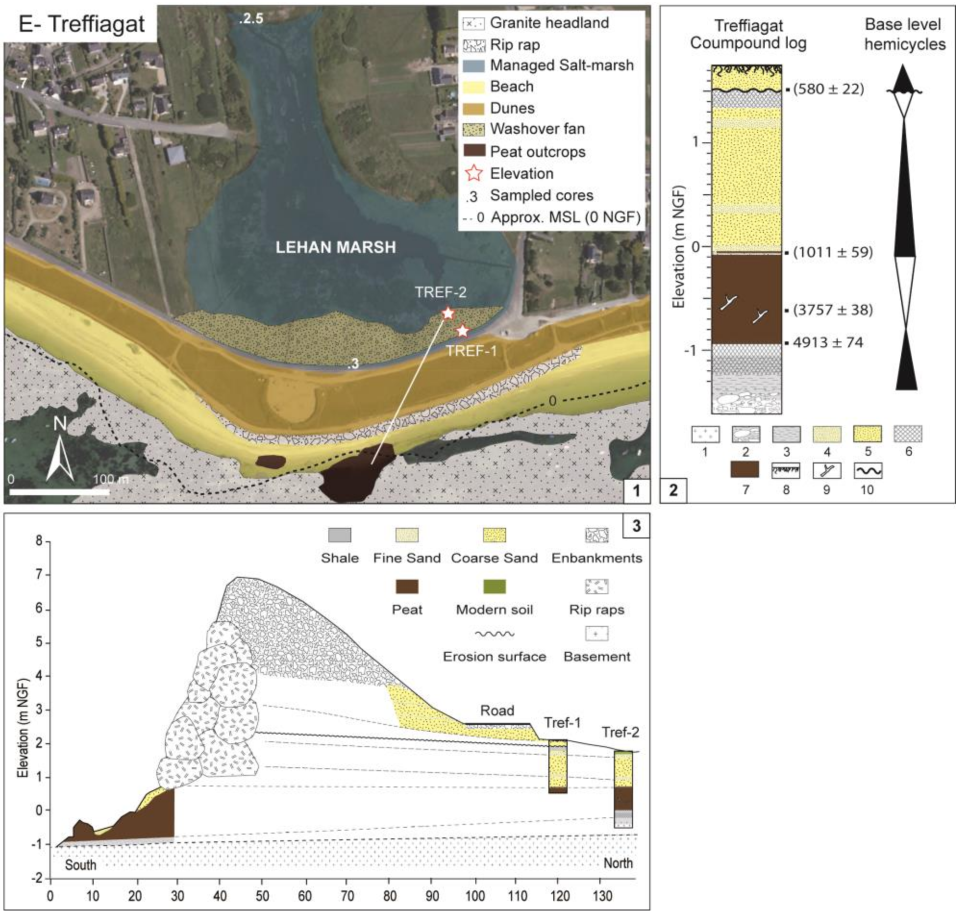

Figure 6 - 1) Map of the Treffiagat site (noted E on Fig.1) showing the location of the TREF-1 and TREF-2 sampled cores (red stars). 2) Detailed stratigraphy from coring transects and trenches/outcrops observations. 3) Compound stratigraphic log of back-barrier sedimentary sequence: 1- Weathered granite basement, 2- gravels and pebbles, 3- Clayey/silt deposit, 4- Medium sand, 5- Coarse sand, 6- Highly organic layer, 7- Peat, 8-Humic soil horizon, 9- wood fragments, 10- Erosion surface.

Commentaire [BVVL5]: NEW FIGURE ADDED

Kermor - Tudy (F. South Finistère)

Two cores were taken in the eastern part of the Kermor site, near the root of the barrier. Core K-IX (3.8 m NF) passed through nine meters of sediments before encountering the weathered basement at

-5.6 m NGF (Fig.7). The base of the sequence consists of a ca. 0.2-m thick silty-peat layer, containing several *Phragmitus australis* and *Juncus sp.* remains. The peat is truncated by a sharp erosive surface on top of which lays ca. 0.5 m of sandy-silt.

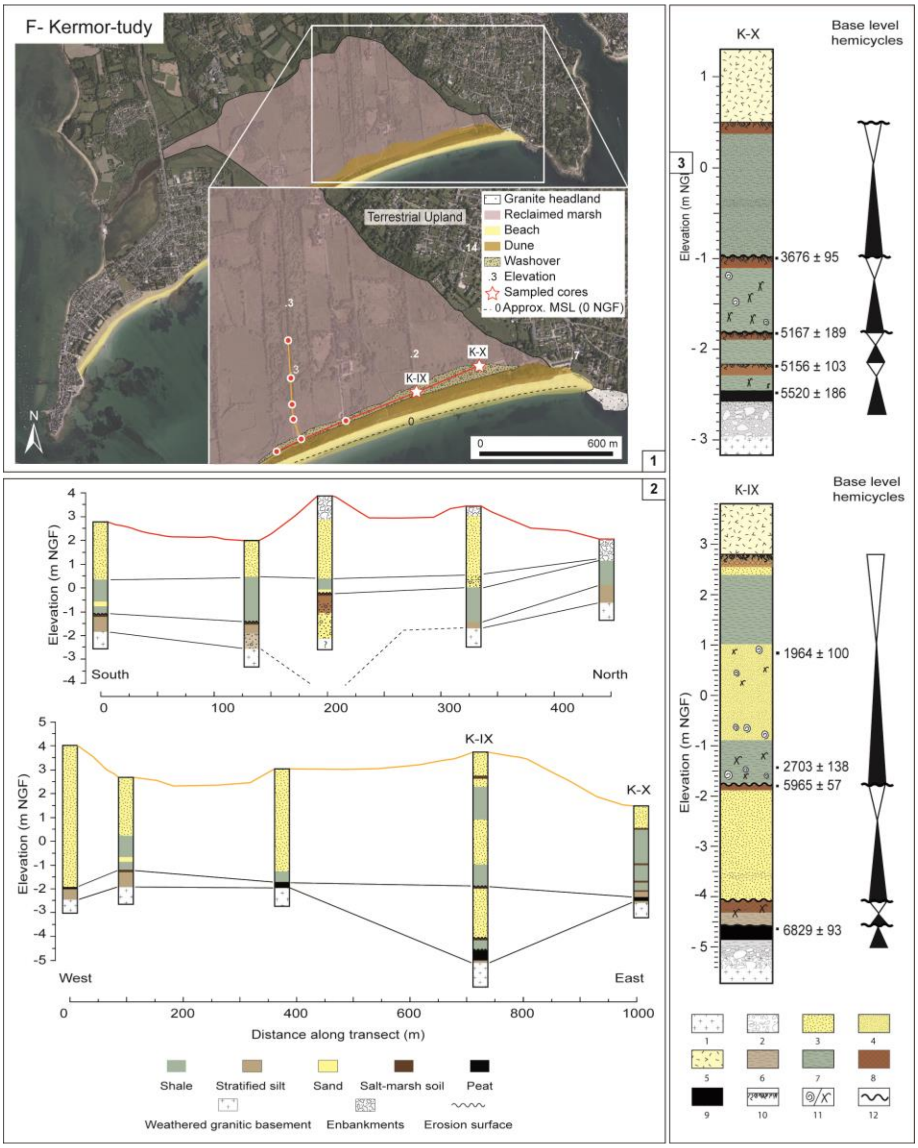

Figure 7 - 1) Map of the Kermor-Tudy site (noted F on Fig.1) showing the location of the coring transects and of the sampled cores (red stars). 2) Detailed stratigraphy from coring transects. 3) Stratigraphic log of the K-IX and K-X sampled: 1- Weathered granite basement, 2- gravels and pebbles, 3- Medium sand, 4- Fine sand, 5- Fine Aeolian dune sand, 6- Organic sandy clay, 7- Sandy clay, 8-Salt-marsh soil horizon, 9- Peat, 10- Humic soil horizon, 11- Shell in living position / fragmented shells, 12- Erosion surface.

Commentaire [BVVL6]: NEW FIGURE ADDED

The top of this latter unit is itself eroded at -4 m NGF and is overlaid by ca. 2 m of slightly shelly coarse sand, topped with a 0.1 m sandy peat layer at -1.8 m NGF. The sequence continues with ca. 3-m thick very-shelly (*Scrobicularia*) sandy-silt infilling.

Above 1-m NGF and up to 2.3m NGF, clay becomes dominant, where it is topped by a 1.5-m thick sand upper layer. Foraminiferas were observed throughout the sequence, but were too scarce to permit representative counting. Assemblages are dominated by *Elphidium williamsoni*, *Haplophragmoides wilberti* and *Haynesina germanica,* which characterize a low-salt-marsh to mudflat depositional environment (Perez-Belmonte, 2008; Stéphan *et al.*, 2014). All dated layers gave geochemical values that are characteristic of the low marsh environment, with populations dominated by *Elphidium williamsoni* and *Haynesina germanica*. Geochemical indicators yielded a heavy $\delta^{13}C$ value of -19.95‰ and very low TOC and TN values (1.17% and 0.11%, respectively) in accordance with a low-marsh environment. Using these latter geochemical values, we obtained a RSL position of -0.67 ± 0.76m on the same layer (index n°3, Table 4).

Core K-X (1.3 m NGF) reached the weathered rocky substrate at -2.7 m NGF (Fig.7). The sequence is composed of a ca. 0.1-m thick sandy silt layer at its base, progressively turning into a black peat until *ca*. -2.45 m NGF (Fig.2). The basal peat was dated using organic content to give an age of ca. 5.5ky cal. B.P. at a depth of -2.49 ± 0.22 m NGF (i.e. ~10 cm above the basal contact). Over the peat lays 0.8 m of very organic stratified silt horizons (Fig.2) cut by a sharp erosion surface. Above this rests a very shelly marine mud layer (*Hydrobia ulvae)*, dated from ca. 5.1 kyr cal. B.P. This layer becomes progressively more organic and looses its shell content towards the top, until *ca*. -1 m NGF where a thin soil horizon is observed. The uppermost part of the core is composed of 1.3 m of brown to green clay, on which rests a dune sand level. The basal peat layer provided geochemical values characteristic of the high-marsh domain. Other samples yielded geochemical signatures characteristic of the low-marsh-to mudflat environment, in accordance with the domination of *Elphidium williamsoni*, *Haplophragmoides wilberti* and *Haynesina germanica* within the foraminifera assemblages. No other indicator bears out a deposition within a brackish environment.

Guidel (E. South Finistère)

Two drillings were completed along a SW/NE transect across the Guidel-Loc'h pond (Fig.8): GLG-1 was drilled in the center of the pond, and GLG-2 was drilled about 500 m seaward of GLG-1.

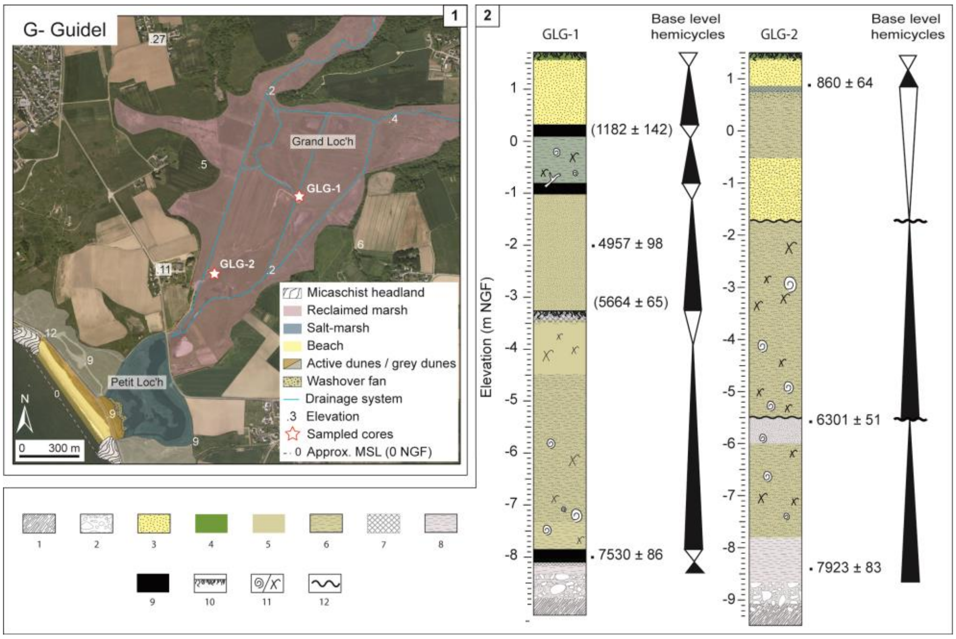

Figure 8 - 1) Map of the Guidel site (noted G on Fig.1) showing the location of the sampled cores (red stars). 2) Stratigraphic log of the GLG-1 and GLG-2 cores: 1- Weathered granite basement, 2- gravels and pebbles, 3- Medium sand, 4- Fine sand, 5- Fine Aeolian dune sand, 6- Organic sandy clay, 7- Sandy clay, 8-Salt-marsh soil horizon, 9- Peat, 10- Humic soil horizon, 11- Shell in living position / fragmented shells, 12- Erosion surface.

Commentaire [BVVL7]: NEW FIGURE ADDED

GLG-1 is an 11-m deep drilling that reached the micaschist weathered basement at -8.3 m NGF. The base of the sequence consists of ca. 0.2 m of lacustrine clay encroaching the basement on which lays a 0.2m thick silty-peat layer. From -7.9 m NGF, the sequence is a 7-m thick succession of sand and muddy-silty layers, interrupted by several salt-marsh soils. The top of the sequence consists of clay-dominated deposits, the uppermost 1.4 m being coarse sand (Fig.8). Except for the basal peat layers, the whole sequence contains foraminifera, the assemblages being dominated by *Haynesina gemanica*, *Amonia becarii* and *Elphidium williamsoni.* At -2m NGF, *Scrobicularia plana* in living position gave an age of 4.9 kyr cal. B.P. Geochemical values infer deposition within a low-marsh to mudflat environment.

The GLG-2 sequence is somewhat equivalent to the GLG-1 sequence, only lacking the basal peat layer (Fig.8). As for GLG-1, the whole sequence is characterized by the extensive presence of shells (*Hydrobia ulvae* especially) within the deposits and by the domination of low-marsh to mudflat foraminifera species.

4.2 Holocene Relative Sea Level variations and responses of the coastal systems

This study has resulted in 24 new dates for the coastal Holocene sedimentary infillings in Western Brittany (table 4). This new RSL record, containing five new base-of-basal SLIPs, considerably improves the precision of the regional RSL history between 8 kyr and 5 kyr cal. B.P. Specifically, (i) this new dataset extends the previous available data by ca.1.5 kyr to 8 kyr cal. B.P.; and (ii) the basal SLIPs provide new critical constraints on RSL inflections around 6 kyr cal. B.P. No reliable basal indexes could be retrieved for dates younger than 4 kyr cal. B.P. so the RSL evolution for the Late Holocene remains less precise (Fig.9). Our new data show an overall continuous 6.5 m RSL rise since 7 kyr cal. B.P. Following an initial rapid rise between 8-6kyr B.P. from ca. -8m to -5m below present-day level, there is a marked slowdown in the RSL rise around 6kyr cal. B.P., after which the rate of RSL rise progressively decreases towards present day values.

4.2.1. RSL evolution from 8 kyr cal. B.P. to 6 kyr cal. B.P.

The two oldest samples (index n° 23 and 24) obtained are intercalated SLIPs and provide for the first time an indication of the RSL history between 8 kyr and 7.5 kyr BP. However, the lack of base of basal peats (Fig.9) limits the reliability of the RSL chronology over this period (Fig.9) These two samples (index n°23 and 24) were obtained from deposits taken at the base of the sequences cored at the Guidel sites but were not sampled directly at the contact with the underlying bedrock. Thus, a compaction-induced artefact cannot be ruled out, and we suspect that true RSL positions may have been slightly higher than drawn by these SLIPs. Therefore, we suggest that the RSL positions given by these two indexes should be taken as indicative of minimum values.

Around 7000 cal. B.P., basal peats formations were emplaced along most of Western Brittany coasts. These basal deposits record a RSL situated between -6.74 ± 1.22m (index n°22) and -6.95 ± 1.22m (index n°20) below present day between ca. 7 kyr and 6.8 kyr cal B.P (Fig.3). A limiting date, obtained from a basal freshwater peat deposit sampled in the Porsmilin sequence (index n°21) further constrains that the RSL was situated *at least* -6.47 m below present-day ca. 7 kyr cal. B.P.

Between 6.5 kyr and 6 kyr cal. B.P., where some SLIPs are derived from incompressible basal peat deposits, there is a continuous RSL rise reaching ca. -3.27 ± 0.76 m at around 5.9 kyr cal B.P. On top of these basal peat deposits, where an erosive hiatuses (wave ravinement surfaces) did not erode the previously-deposited sediments, a widespread onset of silty deposits mostly showing back-barrier lagoonal facies formed. These formations are, in turn, topped by humic layers (maximum- flood surfaces) which suggest a widespread heightening of lagoonal marsh surfaces and evidence for regressive conditions in the back barrier environments. They record the shift from the transgressive system tract towards the mid-Holocene highstand system tract, where deposition most probably occurred in the context of a deceleration of the RSL rise and with a large amount of sedimentary material available within the foreshore domain.

The RSL rise rates we obtained in Brittany between 7ky B.P and 6ky B.P. are closely comparable to those observed for the same period in South-Western UK (Massey et al., 2008, Gehrels *et al.*, 2011; Gehrels and Anderson, 2014), in the North of France (Gandouin, 2003) and in the west of the Netherlands (Hijma and Cohen, 2010), suggesting the eustatic component still played the dominant role in RSL evolution during this period. However, as stated above, due to a lack of basal SLIPs, large uncertainties remain in the RSL rise rates observed in Western Brittany for the older periods.

4.2.2. RSL evolution from 6 kyr cal. B.P. to 4 kyr cal. B.P

From 6 kyr cal. B.P., there is a pronounced slowdown in the rate of RSL rise in Finistère region (Fig.9). Around 5000 yr cal. B.P., basal SLIP n°8 records the RSL at -2.6 ± 0.6 m below the present level, while the high-limiting point n°38 constrains the RSL to lay at least 2 ± 0.55 m below its present position between 4.4 - 3.8 kyr cal. B.P. While the new basal SLIPs clearly suggest a decrease in the RSL rise rate between 6 and 4 kyr cal. B.P., denser and more precise basal data are still necessary to provide a detailed description of this RSL rise deceleration. From a more regional viewpoint, it is interesting to note that, as the rate of RSL rise slowed down, some of our study sites (Porsmilin, Kermor, Guidel) clearly returned to transgressive conditions, as shown by silty-sandy deposits. This stratigraphic evidence implies the local creation of accommodation space between 6 kyr and 5 kyr cal. B.P. driven by (i) the persistent and continuous, even if slow, RSL rise and probably (ii) the possible compaction of the underlying sequences. Indeed, there is a clear spread (up to 3 meters for SLIPs of approximately the same age) of the intercalated SLIPs between 6 kyr and 5 kyr cal. B.P. which is similar to what was observed by Massey *et al.* (2008) in Southwestern UK and by Gandouin (2003) in the St Omer marsh (Northern France). This process may be caused by (i) the onset of coastal barriers due to both a slowing-down in the rate of RSL rise and the large amount of available sediment (ca. 5000 yr cal. B.P.; Van-Vliet *et al.*, 2014a), (ii) by the subsequent landward migration of these barriers, as they rolled-over the back-barrier marsh sequences and (iii) by the shifting of tidal inlets, potentially fostered by barrier breaching (Stéphan *et al.*, 2014).

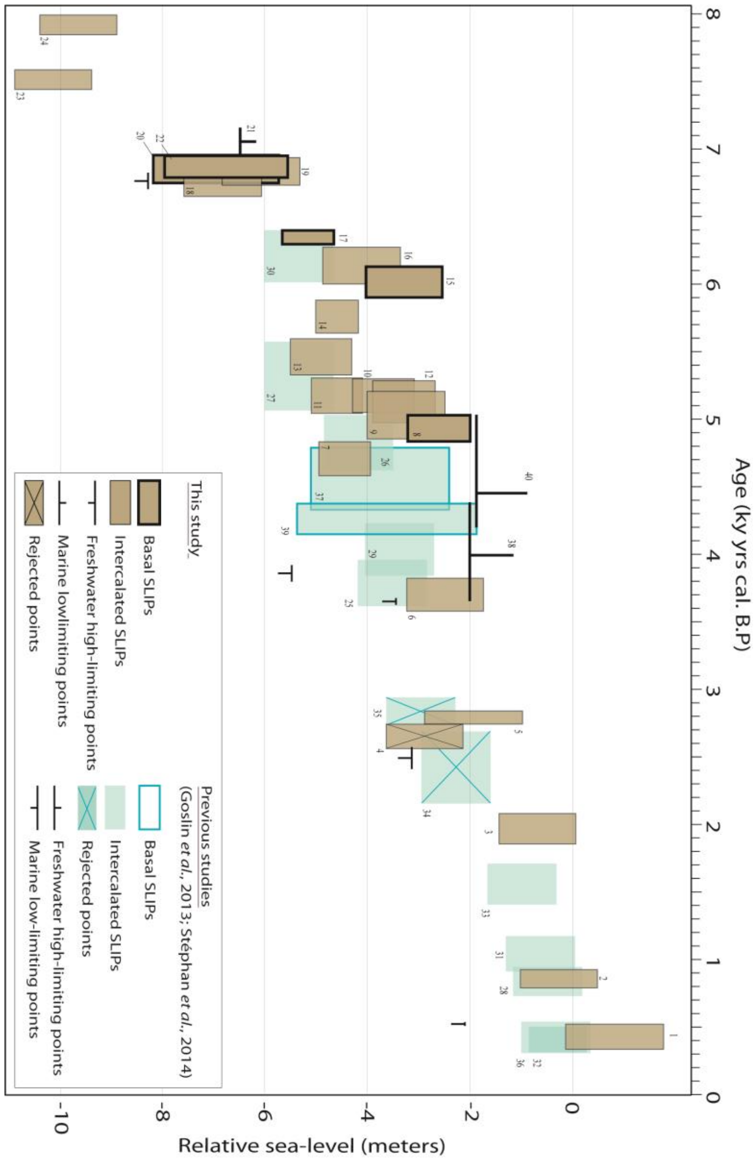

Figure 9 - New Holocene relative sea-level evolution for western Brittany for the last 8 ky cal. B.P. Sea-level indexes are numbered accordingly to table 3 and 4.

4.2.3. RSL evolution from 4 kyr cal. B.P. to present

No basal index-point could be obtained younger than 4 kyr cal. B.P. This, when combined with the lack of SLIPs between 4kyr and 2kyr cal. B.P. (Fig.9), prevents a precise constraint on the RSL evolution during the late Holocene. Several SLIPs that were dated around 3 kyr cal. B.P. (either during this work or by Stéphan *et al.*, 2014) were rejected due to the anomalously low elevation which resulted from a massive reorganization and disruption of the sedimentary system during formation (Goslin *et al.*, 2013, Stéphan *et al.*, 2014), e.g. as illustrated by the widening of the river channel in the Guisseny site.

From 2 kyr cal B.P. onwards, RSL reached a position very close to the present-day. Index n°3 which was obtained from the top of a thick sandy sequence (Kermor KIX) is likely to have undergone only a small amount of post-depositional compaction and hence can be considered as fairly reliable. From this data point, the rate of RSL rise is estimated to have been reached a maximum of 0.71 mm.yr^{-1} during the last ca. 2 kyr cal. B.P. Assuming that the ESL over the last 2 kyr was small, we estimate that Western Brittany underwent a maximum subsidence of ca. 0.7 mm.yr^{-1} for the last 2000 years, as a consequence of the post-glacial isostatic response of the lithosphere. Yet, this value is calculated on the basis of only one point that carries some uncertainty due to its stratigraphical position. Hence, this latter result must be considered as only indicative at this stage of the study and it would require basal SLIPs for the Brittany region over the last two millenaries to be conclusive on this latter point.

Commentaire [BVVL8]: RSL RISE RATES FIGURE DELETED TO FREE SOME SPACE FOR THE FIGURES REQUESTED BY THE REVIEWERS IN THE MODELLING SECTION

4.4 Comparison of Holocene RSL geological records along the English Channel: evidencing for a particular behavior of south-western UK (Devon, Cornwall and Scillies).

Commentaire [BVVL9]: COMPLETELY REWRITTEN SECTION

Vink et al. (2007) gave clear evidences for the glacio-isostatic subsidence induced by the collapsing of the northern Europe peripheral bulge to progressively decrease along a NE- SW gradient running from Germany to Belgium (as mainly driven by the loading of the FIS). In order to explore the glacio-isostatic gradients and subsidence patterns induced by the loading of the north-European ice-sheet complex and the collapse of associated peripheral bulge, we compared the RSL data from this study to the high-quality RSL records available along the English Channel, either produced by the study of Holocene sedimentary successions in Southwest UK (Devon, Cornwall and Scillies, Healy, 1993; Healy, 1995; Massey *et al.*, 2008; Gehrels *et al.*, 2011, Gehrels and Anderson, 2014), southern UK (Hampshire region; Long and Tooley, 1995), Northern France (Seine Estuary, Huault, 1980; Frouin *et al.*, 2007; Stéphan and Goslin, 2014) and Belgium (Izjer valley, Denys and Baetman, 1995). The main aim of this comparison was to broadly evaluate if the glacio-isostatic subsidence gradient identified by Vink *et al.* (2007) from northern Germany to Belgium could be followed further eastward.

As far as the data allowed it, only the basal SLIPs were compared. Before the data could be compared, adjustments had to be made to fix vertical differences between the datums of the different countries and/or the RSL datum used within the different studies. Indeed, the French data are referenced to the NGF system (Nivellement Général de la France) at Marseilles (IGN69 datum), the UK data we used are related to the Ordnance Datum of Newlyn (ODN) while the Belgium data is related to the DNG system (Deuxième Nivellement Général) at Ukkle. Yet, the ODN is higher than the NGF of ca. 40 ± 2 cm (Greaves *et al.*, 2008), while the Belgian DNG lies 1.75m above the NGF (Crastes de Paulet, 2013). Hence*,* before comparing the different RSL datasets, we applied a consistent altitudinal correction to the depths of the samples to resolve this altitudinal discrepancy: a ca. -40 cm shift was applied to the UK RSL data prior to their comparison with our RSL records, while the Belgian data were lowered by 1.75m. However, as for the ODN correction it must be noted that this offset is a somewhat crude estimate and is likely to slightly overestimate the real difference between both datum's. Nonetheless, considering the fact that leveling errors are globally east-west conservative both in UK and in France (Rebischung *et al.*, 2009), this correction can be considered as a sufficient first approach (P. Woodworth, *comm. pers,*). In some of the UK studies we took data from (Massey *et al.*, 2008), RSL positions were expressed relative to MTL, and not to ODN. In order to relate these data to ODN and prior to the correction for the vertical difference between the ODN and NGF datum, these were applied them a vertical shift corresponding to the local tidal heights relative to ODN (Massey *et al.*, 2008): -0.11m, -0.09m, -0.12, -0.11 for the SLIPs obtained at Bantham Sand, North Sands, Slapton Sands and Blackpool Sands sites, respectively.

This comparison clearly shows that all studied regions undergone very comparable RSL histories during the 8.5 - 5 ky B.P. period, in great accordance with the one of Western Brittany. While all regions seem to have experienced slightly different RSL variations over the considered period (that is notably observable via slight differences in the RSL rise rates prior to 5 kyr cal. B.P.), a general synchronicity is clearly observable between the RSL trends estimated from the records. In all regions, there is an obvious inflection in the rate of RSL rise at ca. 6 kyr cal. B.P. (Fig.10) that most probably reflect a decrease in meltwater production from the melting of the global ice sheets (Vink et *al.*, 2007).

The synchronicity of the global RSL trends between Brittany and sites located eastward (Hampshire, UK; Seine Estuary, Northern France) in the English Channel and at its eastern termination (Izjer Valley, Belgium) suggests that all considered regions have been subjected to major synchronous RSL forcing agents.

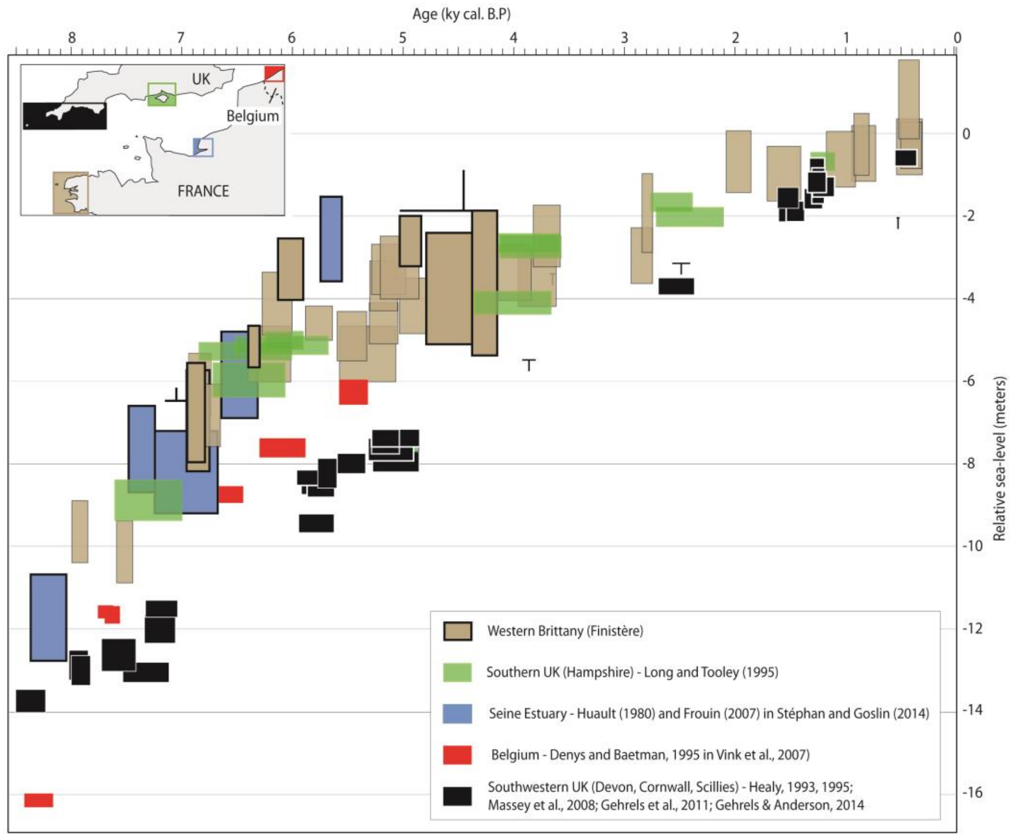

Figure 10 - Inter-regional comparison of RSL records from Western Brittany (brown boxes), South-western UK (Devon, Cornwall - black boxes), Central UK (Hampshire - green boxes), Seine estuary (Blue boxes) and Western Belgium (red boxes) during the last 8 ky B.P. Mind that all represented data basal SLIPs, excepted thin contoured brown boxes and SLIPs from Hampshire. These latter may thus have been lowered by some post-depositional compaction and hence potentially underestimate RSL position.

Commentaire [BVVL10]: NEW FIGURE ADDED

The RSL record from Belgium plots several meters under the ones from the Seine, Hampshire and Brittany regions (Fig.10). This undoubtedly illustrates the greater subsidence undergone by the Belgium coastal plain, in relation to the collapse of the peripheral bulge situated at the south of the North Sea (Vink et al., 2007). Indeed, this latter region has most probably been subjected to the conjunction of two subsiding dynamics, coming both from the north (glacio-isostatic gradient linked to the collapse of the peripheral bulge south of the BIIS, as evidenced by Horton and Shennan, 2009) and from the north east, induced by the deflation of the peripheral bulge southwest of the FIS (Vink et *al.*, 2007). Progressing westward, we note that the Hampshire and Seine regions show very lookalike RSL records. Being located both in the middle part of the English Channel and in very comparable in regard to the North Sea and Atlantic basins, these two regions must have been subjected to a somewhat equivalent hydro-isostatic component, yet difficult to evaluate at this stage of the study. This high variability in the hydro-isostatic component associated with the relatively large error margins the SLIPs are weighted with makes it difficult to precisely identify a glacio-isostatic gradient that potentially progressively damps westward along the English Channel.

However, a spectacular result emerges from the visual comparison of the RSL records that shows the RSL data from SW UK to plot consistently several meters below the data of all studied regions during the last 8 kyr B.P. Indeed, before 5 kyr cal. B.P the basal SLIPs retrieved from SW UK sedimentary sequences SLIPs plot ca. 4 meters below the ones we obtained in Brittany (Fig. 10). It is interesting to note that the offset seems to reach a maximum ca. 6-5 ky B.P., while it appears to decrease towards the older and younger times. To the first order, and assuming a constant decrease of the isostatic component, Brittany would have subsided at an average rate between 0.42 and 0.67 mm.yr$^{-1,}$ since 6 kyr cal. B.P., while the subsidence over the same period reached 1.3 to 1.5 mm.yr^{-1} in Devon (a lack of basal data for Brittany after 6 kyr cal. B.P. precludes a similar comparison for the late Holocene period). This result is especially revealing if we consider that Brittany and SW UK have subsided partly in response to the loading of the continental platform: the hydro-isostatic component accounts for ca. -2 to -3 m since ca. 7 kyr cal. B.P. and is considered commensurate between the two regions (e.g. Leorri *et al.*, 2012) as these latter share comparable peninsula configurations and almost identical geological histories and features. Investigations on the gravitational and solid Earth changes from 10 kyr cal. B.P. show the geoid being less than 0.5m higher for Brittany than for Devon/Cornwall at 8 ky cal. B.P. Therefore, the influence of differing hydro-isostatic components seems unlikely to explain the large vertical discrepancies observed between UK and Brittany RSL levels.

In spite of the larger uncertainties concerning the most ancient and the most recent periods, this result nonetheless confirm that a time-dependent north-south subsidence gradient seems well to exist along the Atlantic coasts of Europe. This gradient would result from the collapse of the peripheral bulge of the European ice complex (British-Irish and Fennoscandian Ice-Sheets). SW UK and Brittany being located at equivalent distances from the centers of glaciations, it could be awaited from glacio-isostatic component to be broadly equivalent in the two regions and RSL histories to be quite close. As it is not the case, we believe that two main hypotheses can be put forward. One hand, our new findings may challenge the inferences previously made on the amplitude and extent of the peripheral bulge of the north-European Ice-sheet complex south of the BIIS. The amplitude of the vertical offsets observed between Western Brittany and Southwest UK RSL records could imply that Devon was much closer to the apex of the bulge than Western Brittany was. If this is the case, our new findings challenge the inferences previously made on the amplitude and extent of this bulge. The offset amplitude in the isostatic subsidence between Brittany and Devon, regions which are close to one another, would suggest some combination of (i) a shorter wavelength of the bulge than was previously inferred by Lambeck (1997) and Leorri *et al.* (2012) and of (ii) a more northern position of the bulge apex than was previously considered. One another hand, differences in the Earth response are also likely to be invoked to explain such an offset. These results are in favor of a geological origin for the still unexplained differences in the land-subsidence rates obtained from tide-gauges records between Brest and Newlyn, as already suggested by Woodworth (1987). Indeed, recent tide-gauge based modern RSL studies (Wöppelmann et al., 2006, Douglas et al., 2008, Haigh *et al.*, 2009) suggest that RSL rises at a rate of 1.74 mm.yr^{-1} at Newlyn against 1.41 mm.yr^{-1} at Brest, thus advocating for a greater subsidence in SW UK.

4.5 Comparison between predictions from GIA Models and RSL observations in Western Brittany.

Commentaire [BVVL11]: RE WRITTEN SECTION WITH SUPPLEMENTARY FIGURES : 1) RSL SPATIAL PLOTS

To investigate more in depth the origins of the vertical discrepancies we identified between Brittany's and south-western's UK RSL records, we compared the new RSL data obtained in Western Brittany (this work) and GIA model RSL predictions. As no significant differences could be identified between the data records from the northern and southern part of our study area, we chose the location of Guisseny (the northernmost site of our study area; 48°65' lat, -4°45' long.) as the reference location for data-model comparison. This choice pertains to the fact that most of the basal SLIPs we obtained come from the northern coast of Brittany. It is also justified by the fact that all sites that produced basal SLIPs are seen to have been concerned by an equivalent hydro-isostatic component during the last millenaries.

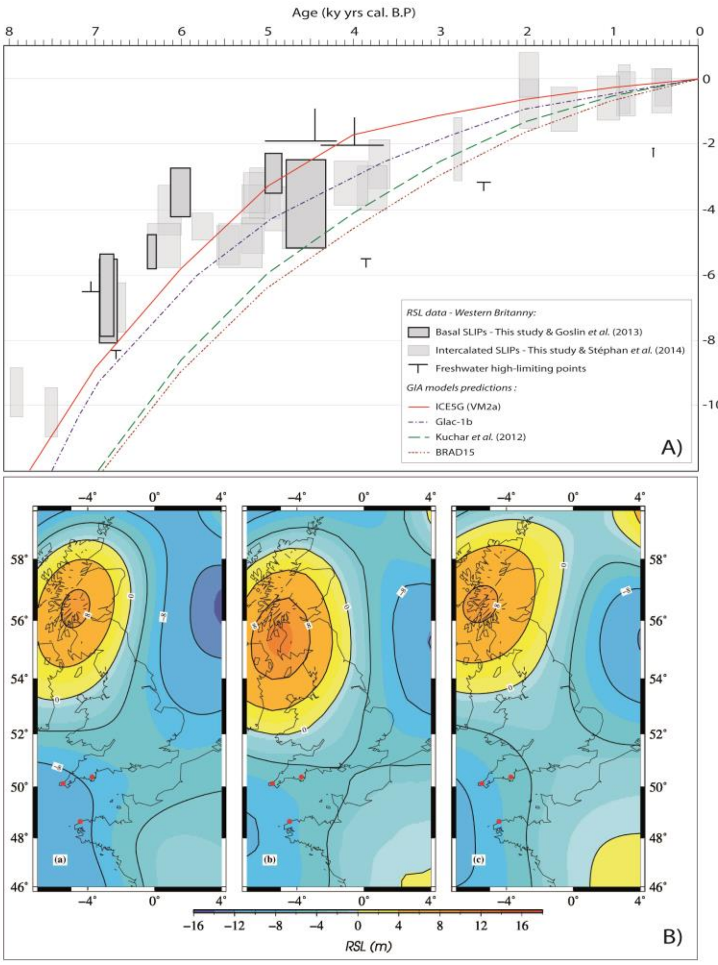

Figure 11 – A) Data-model comparison between Holocene RSL observational data for western Brittany (this study - grey boxes) and RSL predictions produced by GIA models of global and regional significance (color lines), B) Spatial plots of the RSL evolution as predicted by the BRAD15, GLAC-1B and ICE-5G VM2a GIA models, respectively. Here is shown only the RSL plot at 6 ky B.P. Plots for 7, 5 and 4 ky B.P. periods can be found in the SOM (Appendix 3).

Commentaire [BVVL12]: NEW FIGURE : RSL Spataila plots to illustrates the spatial differences between the different models' predictions

From the data-model comparison there are some key points (Fig.11):

- The patterns of the RSL predictions from the various models are, in general, consistent with our observations. The predicted RSL trends approximately capture the inflections in the observed rate of RSL rise at ca. 7, 6, 5-4 and 2 kyr cal. B.P. (Fig.11)

This synchronism validates *a posteriori* the global pertinence of both the ICE-5G, BRAD15 and GLAC-1b multiple ice models chronologies used as inputs for GIA models.

- However, none of the models, whether “global” or “regional”, was able to fit accurately our new RSL observations in Brittany. All models under-estimate observed RSLs by up to several meters for the last 8 kyr and thus either (i) infer inaccuracies in the timing and amount of melt from the global ice sheets or (ii) over-estimate the peripheral bulge subsidence. For example, the predictions of the ICE-5G (VM2a) and GLAC1-b models lay up to 3 m below the mean RSL position obtained from our basal SLIPs at 7 kyr cal. B.P. (Fig.11). When the "regional" “BIIS” and Kuchar *et al.* (2012) models are compared to our new data, the misfits are even larger, ca. 6 m around 7 kyr cal. B.P. and more than ca. 2 meters around 4 kyr cal. B.P. (Fig.11). The global ICE-5G (VM2a) model, which is the most highly tuned (of the models sampled) to fit global RSL data, is the one that produced the best fit to our observations. Conversely, the best-fit UK regional models fail to fit our new RSL data. These latter models produce RSLs for Brittany which plot slightly below those they produce for Devon. It was previously proposed (Lambeck *et al.*, 1997; Leorri *et al*., 2012) that the two regions would have undergone comparable amounts of glacio- and hydro-isostatic subsidence, with Devon subject to a slightly stronger glacio-isostatic signal. Our new data reinforce this idea but suggests a more abrupt damping of this component across the Channel.

4.6. Evaluating the influence of local process: changes in the paleo-tidal ranges

As stated before, we investigated changes in regional tidal ranges so that our RSL data, constructed from high-tide indicators, could be directly compared to the RSL predictions from the GIA models. For each of our sites, changes in the neap, spring and maximum annual tidal ranges are shown in appendix S2 as height values and percentages of the present-day ranges. Graphical representations of the results are presented in figure 7. The results of the paleo-tidal modeling indicate that there were only very slight changes in the tidal range at our study sites during the last 8 kyr. The maximum changes occurred between 8 and 6 kyr cal. B.P. and are mainly driven by changes in the neap tidal ranges. For these latter, maximum changes were observed for the southern sites of our study area (Treffiagat, Guidel), where neap tidal ranges increased by up to 30% of the present-day value between 8 and 6 kyr cal. B.P. before reaching their present day values ca. 6 kyr cal. B.P.

However, considering the reduced amplitude of the tidal ranges at these sites, these tidal increases only represent ca. 50 cm changes in height values (25 cm in half tidal ranges). Different evolutions were observed for the spring tidal ranges. Indeed, for most of the sites situated on the outer coasts of our study region (i.e. Bay of Brest and entrance excluded), model runs suggest that spring ranges reached a maximum at 6 kyr cal. B.P., with values greater than present-day by to up to 3 to 6%. This only translates into minor changes in the height values (max. 0.3 m). More importantly, the relationships between neap, spring and astronomical tidal ranges have remained very constant through time on all our study sites (see SOM, appendix S2). As a consequence, only minor changes in indicative ranges are applied to most of the extracted SLIPs (Figure 14). Additionally, the model results show differences between neap and maximum tidal ranges to have continuously increased since 8 kyr cal. B.P., the most important rise being observed for Guisseny (0.7m). These changes required the indicative ranges of SLIPs derived from undifferentiated high-marsh brackish peat deposits (see section 3.1.3, indexes n°20, 22 and 39) to be slightly adjusted (reduced by 0.09m). As a main result, we can state that our HWST-related indicators lead to only slightly over-estimate the MSL evolution. Yet, it must be noted that the paleo tidal models we used were developed at a regional scale (continental shelf) and thus are most probably unable to catch the changes in tidal ranges that may have occurred at site-scales due e.g. to reorganizations of the foreshore sedimentary wedges. These local changes in tidal ranges may have potentially been higher than those we modelled at the shelf-scale.

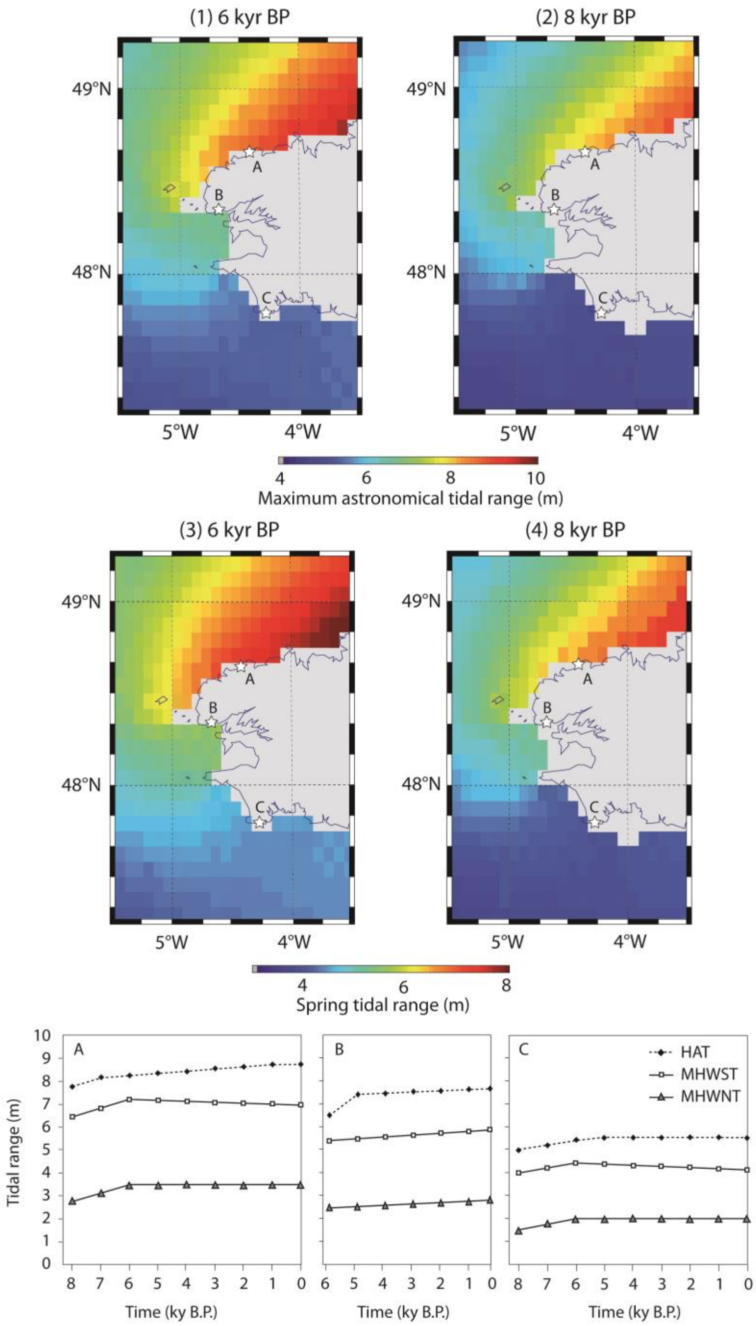

Figure 13 - Paleo tidal model outputs of the maximum annual tidal range (maps 1 & 2) and Spring tidal ranges (maps 3 & 4) for the study region for 8 ky and 6 ky cal. B.P. Stars show the locations of the Guisseny-Tressény (A), Porsmilin (B) and Treffiagat (C) sites. Example plots of the 8ky to present-day evolution of the local max. annual, spring and neap tidal ranges are shown. Plots for the other sites are given in SOM (appendix S2). Complete model outputs values can be found as supplementary material in SOM (appendix S2).

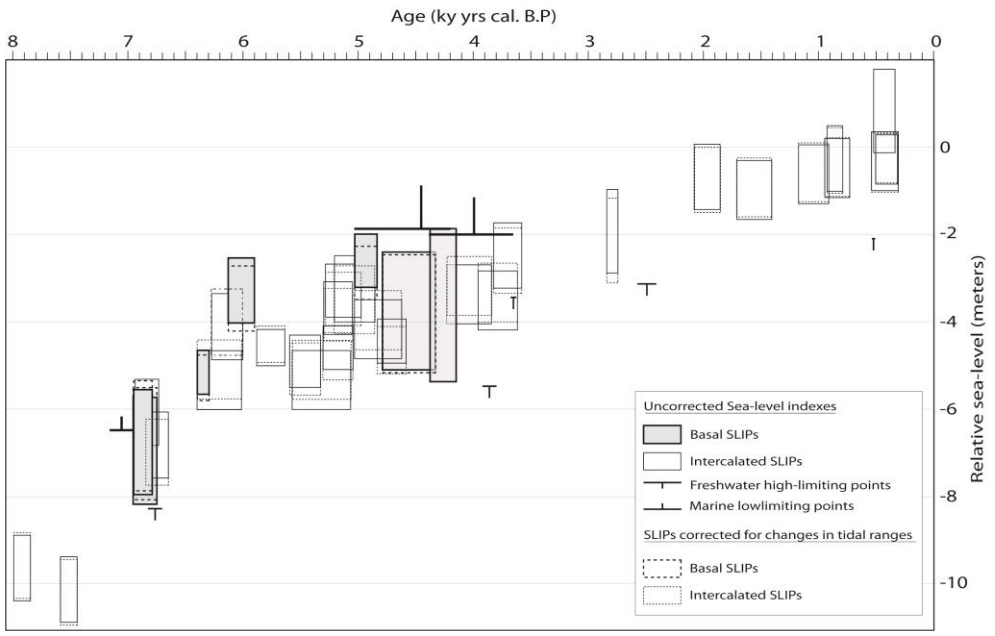

Figure 14 - Sea-level index points uncorrected (plain boxes) and corrected (doted boxes) for paleo tidal range changes through the last 8 ky cal. B.P.

4.7. Regional to global causes of the data-models misfits: North-western Europe Ice-sheet complex history, lateral variations in the earth structure and meltwater contributions

Commentaire [BVVL13]: RE WRITTEN SECTION WITH SUPPLEMENTARY FIGURES : 1) PLOT OF SPLIT RSL SIGNALS BETWEEN REGIONAL AND FAR-FIELD ICE-SHEETS ADDED TO FIG.9, 2) PLOTS OF SENSITIVITY ANALYSES TO EARTH-MODEL PARAMETERS

As demonstrated above (section 4.4), the effects of regional changes in the tidal-ranges remained negligible during the Holocene in our study region and are largely insufficient to explain the plurimetric offsets observed between our observational RSL data and GIA models RSL predictions (Fig.11, Fig.14). As such, hypotheses other than local to regional changes in the tidal ranges are required to explain the large data-models misfits we observe. In this section, we explore several agents that may play a role in the data-models misfits we observe between the RSL predictions of the GIA models and our RSL reconstruction based on geological indicators.

We propose that the misfits could mainly be due to an over-estimation of the glacio-isostatic component, which can be explained by an over-estimation of the spatial extent and amplitude of the European peripheral bulge and/or to temporal inaccuracies. This is partially corroborated by the increases in model/data misfits with time. The easiest solution to resolve such under-predictions could be to lower the vertical amplitude of the peripheral bulge, e.g. by reducing the ice-thicknesses - and hence ice-loads - over the British Isles. Yet, a thinner BIIS would considerably increase the model-data discrepancies in near-field areas (such as Scotland) and would be contrary to the recent reevaluations of Scottish trimline data. Indeed, these latter studies suggest that BIIS ice-thickness would have conversely been thicker than what is accounted in the models we used (e.g. Ballantyne *et al.*, 2008, Ballantyne, 2010; Ballantyne and Stone, 2015). To investigate the sensitivity of the RSL predictions to the size of the BIIS, we generated RSL predictions for the Brittany region with bounding variants of BIIS ice models (i.e., various ice-thicknesses for the BIIS, figure 9a and 9b). For example, the revised ice-model used by Kuchar et al. (2012) which is up to two-three times thicker than the BRAD15 ice model (Bradley *et al.*, 2011) only results in a maximum 0.5 m vertical difference in the RSL predictions produced by the two models (Figure 9a). This statement is also supported by figure 9b, where RSL predictions generated by the GLAC1-b model with extremal bounding BIIS variants (bounding with respect to regional Holocene RSL). These results illustrate that diverging scenarios of the BIIS and ice-thicknesses over the British-Isles would only be responsible for slight changes in the RSL predictions for ice-distal locations such as the Brittany region. As we illustrated in figure 9 and already suggested by Bradley *et al.* (2011) and Kuchar *et al.* (2012), the RSL signal at these distal southern sites is primarily driven by eustasy and the collapse of the peripheral bulges from all the major Northern Hemispheric ice-sheets, and most prominently that of the Fennoscandian ice sheet that accounts for much of the loading within our study region (about 50% at 6 ky cal. B.P., Fig.9 and Fig.10). This advocates for the data-model misfits observed for Brittany, if such misfits are well driven by problems at the level of the architecture and deglaciation histories of the ice-sheets, to be rather linked to FIS than to BIIS. GIA response being non-linear, in must be noted that the separation between ice-sheets would be fully appropriate only neglecting the migration of shorelines. The results of such a separation are only approximations. Yet, uncertainties linked to this phenomenon are likely to be very small, causing changes in the RSL trends of an order of $2x10^{-6}$ $mm.yr^{-1}$ (G.Spada, *comm. pers.*) Finally, the complex trade-of between regional and global signals must be accounted that makes that straightforward relationships between ice-thicknesses and RSL history of distal regions remain hard to establish (Kuchar *et al.*, 2012).

On the basis of such statements, we suggest that the possible origin for the data-model discrepancies are related to some combination of: (i) errors in the regional earth structure in the adopted Earth model, (ii) inaccuracies in the pattern of ESL due to potential issues related to the amplitude, provenance and timing of farfield meltwater contributions and (iii) issues relating to the spatial and temporal pattern of deglaciation of the FIS and LIS and the resultant peripheral bulges.

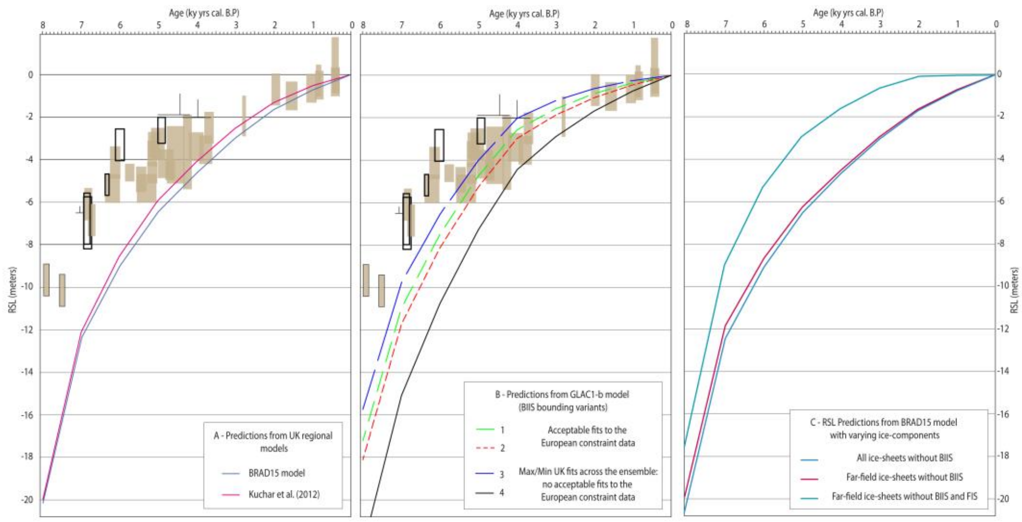

Figure 9 - (A), (B) Plots showing the effects of varying the British Irish Ice-Sheet on the RSL predictions from the regional and global GIA models, respectively (refer to the text for further explanation). (C) Plot of the RSL signal induced by the different ice-sheet loadings as predicted by the "BIIS" model, showing the relative responsibility of far-field ice-sheets, BIIS and FIS within the total Holocene RSL signal for the Brittany region. (A) Predictions from the regional models fine-tuned for the British-Isles. "BIIS" and Kuchar models ran with a unique earth model (lithosphere thickness of 71 km, upper- and lower-mantle viscosity of 0.3×10^{20} and of 2×10^{20} Pa.s, respectively). Note that the BIIS in the Kuchar model is 2-3 times than in the "BIIS" model (B) Predictions of the Glac1-b model for BIIS bounding variants (after 9087 full model runs): Inner curves (red and green lines, respectively) do have weakly acceptable European Ice-sheets. Conversely, outer curves (black and blue lines, respectively) show max/min UK fits across the ensemble and do not have acceptable fits to the European constraint data.

With regards to rheological issues, the data-model discrepancies we observe may originate from the fact that most GIA models use radially-varying one dimensional Earth models that assume a spherically symmetric Earth rheology. Yet, such earth models have been shown to be inaccurate (e.g. Spada *et al.*, 2006; Whitehouse *et al.*, 2006) as they disregard lateral variations in the Earth structure. The VM2 and VM5a earth models, which were combined with the ICE-5G and Glac-1b global models were developed on the basis of the fit to RSL data from old-cratons regions of north-American (Hudson Bay, Canada) and Northern-Europe (Angerman River, Sweden). Hence, these models do not consider the large-scale variations in the earth structure that were identified at the scale of Western Europe (Spada *et al.*, 2006; Whitehouse *et al.*, 2006) and also may not be appropriate to use at locations distant from the reference regions to which they were tuned.

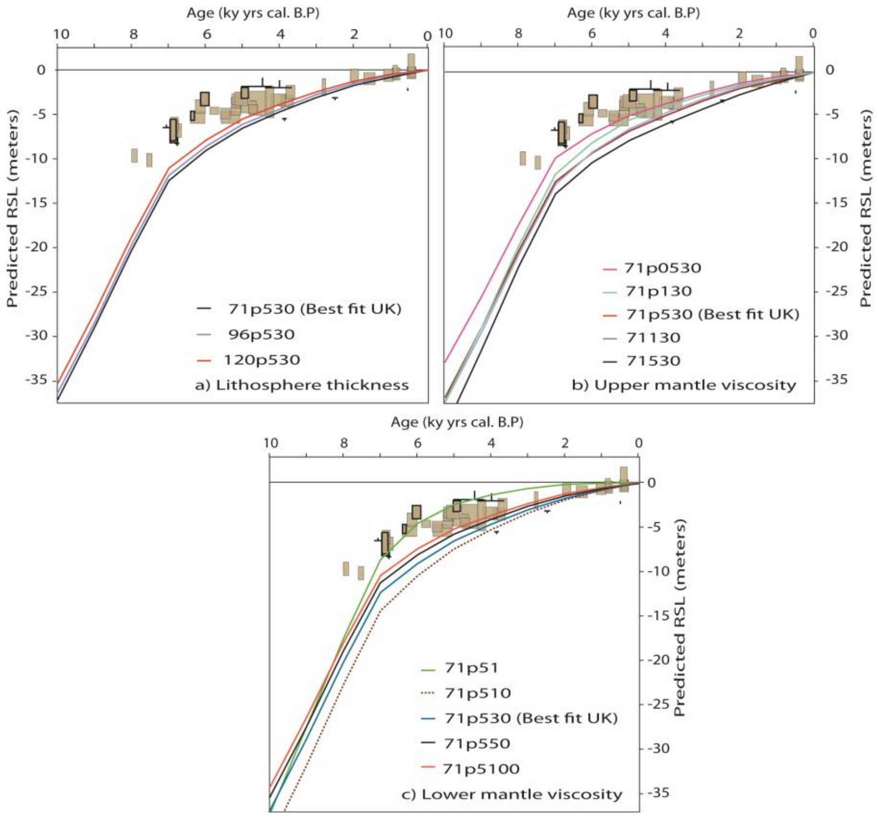

Figure 10 - Plots of "BIIS" model RSL predictions for a range of (a) varying lithosphere thicknesses, (b) varying upper mantle viscosities and (c) varying lower mantle viscosities. In (a), 120p530, 96p530 and 71p530 are model predictions for lithosphere thicknesses of 120 km, 90 km and 71 km, respectively and fixed upper- and lower-mantle viscosities of $5x10^{20}$ Pa.s and $3x10^{22}$ Pa.s (parameters of the best fit model for the British Isles, Bradley *et al.*, 2011), In (b) 71p0530, 71p130, 71p530, 71130 and 71530 are predictions for fixed lithosphere thickness and lower mantle viscosity values of 71 km and $3*10^{22}$ Pas, and upper-mantle viscosities values of $5x10^{19}$ Pa.s, $1x10^{20}$ Pa.s, $5x10^{20}$ Pa.s, $1x10^{21}$ Pa.s and $5x10^{21}$ Pas, respectively. In (c) 71p51, 71p510, 71p530, 71p550 and 71p5100 are predictions for fixed lithosphere thickness and upper- mantle viscosity values of 71 km and $5x10^{20}$ Pa.s, and lower-mantle viscosities values of $1x10^{21}$ Pa.s, $1x10^{22}$ Pa.s, $3x10^{22}$ Pa.s, $5x10^{22}$ Pa.s and $10x10^{22}$ Pa.s, respectively.

Commentaire [BVVL14]: NEW FIGURE

The best-fit UK regional models ("BIIS" and Kuchar) were also combined with Earth-models that adopt only a spherically symmetric Earth rheology (Bradley *et al.*, 2011, Kuchar *et al.*, 2012). However, these Earth model parameters were fine-tuned to provide adequate regional solutions fitting UK RSL data and UK GPS data. In this context, the very large misfits we observe in Brittany between the data and the UK regional models are even more surprising and we propose three possible explanations.

First, regional models were tuned to an older, relatively poorly constrained FIS component (modified from ICE-3G model, see Shennan *et al.*, 2006), which would in turn affect the amplitude and/or position of the European peripheral bulges. Yet, as stated before, FIS would drive most of the RSL signal for the NW Europe sites. Another explanation could be that adopted regional earth model parameters are biased towards the RSL data from the northern rather than southern site (see Fig.7c and Fig.4c in Bradley et al, 2011 and Kuchar 2012). Indeed, these studies showed a clear distinction in the sensitivity of the RSL data to the adopted Earth model parameters between the northern and southern UK RSL data. Finally, an explanation could be related to the lateral heterogeneities in the lithospheric structure and mantle viscosity profile across the English Channel that are not included within the earth models. We made some tests to evaluate the dependency of the data-model misfits to changes in the Earth parameters (Fig.10). Several combinations of lithosphere thicknesses and upper- / lower-mantle viscosities were ran within the BRAD15 model. Slight variations in the RSL predictions are with the different lithosphere thicknesses, in accordance with the suggestions of Watts (2001) and Whitehouse *et al.* (2006). One another hand, our results show RSL predictions from BRAD15 model to be particularly sensitive to changes upper- and lower-mantle viscosities. The best fits with RSL data from Brittany are obtained with low upper- and lower-mantle viscosities of $5x10^{19}$ Pa.s and $1x10^{21}$ Pa.s, respectively. Those viscosities are significantly lower than those of the best-fit model for the British Isles (Bradley *et al.*, 2011; Kuchar *et al.*, 2012), thus possibly highlighting for large lateral variations in the Earth structure across the Western termination of the English Channel. Such variations seem supported by seismic tomography studies which find evidence for differences in the lower upper-mantle shear wave velocities between France and south-western UK at 410 and 585 km depths (Legendre *et al.*, 2012; Zhu *et al.*, 2012). Particularly, contrasts in the S-wave speeds of up to 4% are observed in the Western and Irish Sea regions, which can be converted into variations in the upper mantle viscosity of up to four orders of magnitude (Wu *et al*.; 1998) between Cornwall-Devon and Brittany. This evidence supports the theory that significant variations exist in the near-field lateral structure of the shallow earth below the study regions, which are not resolved by the GIA earth models. This said, a caveat must be that such low upper-mantle viscosities values are inconsistent with Angerman river decay time constraints (Nordman *et al.*, 2015) (**Can you develop, LEV??**). Finally, the presence of a deep relic crustal suture zone (Rheic suture) along the southern coast of England (Legendre *et al.*, 2012) also raises the question of the likelihood for the elastic response of the lithosphere to get mitigated in the vicinity of deep faulted suture zones.

Commentaire [BVVL15]: NEED SOME HELP HERE TO WRITE SOMETHING SUBTLE AND PRECISE.

Also, As all GIA models considered under-estimate the RSL during the older Holocene (pre 8 kyr cal. BP), this would be consistent with an under-estimation of the ESL resulting from the far-fields ice sheets, such as Antarctic, Iceland, Patagonia and Eastern Siberia / Artic sea during this period (Clark & Tarasov, 2012; Niessen *et al.,* 2013). As originally proposed by Milne and Peros (2013) from comparisons with RSL data from circum-Caribbean far-field regions, the fact that the predictions of Bradley's and Kuchar's models fall far below our observational data may imply that the EUST3 global model (part of the BRAD15 model; Bradley, 2011, Bradley *et al*., submit.) used by these models involves too much melting after 8 kyr B.P., in turn causing the "eustatic" component to be over-deepened during Mid- to Late-Holocene. However, an increase in the melt from 8 kyr BP was required in the EUST3 model to reduce the over prediction in the height of the Holocene high stand at the UK and Ireland RSL data.

Conclusion

This new RSL dataset developed for the Finistère region (Western Brittany, France) significantly improves our knowledge of the Holocene RSL history in this region. We observe a general ca. 7-m RSL rise over the last seven thousand years. The six new basal SLIPs, free from possible vertical displacement induced by post-depositional compaction, now enable the extraction of reliable RSL trends for the 8 kyr to 4 kyr B.P. interval. These new SLIPs points more precisely constrain the decrease in the rates of RSL rise during the Mid-Holocene, with inflections centered around 7 kyr, 6 kyr and ca. 5-4 kyr cal. B.P. During Late Holocene (post 4 kyr cal. B.P. period), the lack of basal data still precludes the reconstruction of a precise reliable RSL history. This study, for the first time applies paleo-tidal modeling corrections to SLIP reconstructions for data sites from France. The results of our paleo-tidal modelling confirm those previously published by Uheara *et al.* (2006) and Neill *et al.* (2010), showing (i) that tidal ranges only underwent slight changes since 8 kyr cal. B.P. (max. 0.7m increase) and (ii) that the relationships between neap, spring and astronomical tidal ranges remained very constant through time.

This revisited Holocene RSL evolution for Western Brittany has significant implications for the understanding of isostatic dynamics along the Atlantic coasts of Western Europe and, particularly, of its glacio-isostatic component, linked to the collapse of the European peripheral bulge south of the British Isles. A large time-dependent vertical offset between the RSL records of the two regions suggests that Southwestern UK experienced a greater subsidence than Western Brittany during the last thousand years. We propose, that this offset probably indicates that Southwestern UK was located closer to the apex of the bulge than Brittany was.

At a larger scale, our results challenge the hypotheses that were previously proposed on the amplitude and the extent of the glacio-isostatic peripheral bulge subsidence along the Atlantic coasts of Northwestern Europe. Comparisons of our data with RSL predictions from both global ICE-5G (VM2a) and GLAC1-b (Tarasov & Peltier, 2002; Tarasov *et al.*, 2012; Briggs *et al.*, 2014) and regional ("BIIS" model of Bradley *et al.*, 2011, model of Kuchar *et al.*, 2012) GIA models show that none of the models fit our observations satisfactorily. The regional models under-estimate the observed RSLs by several meters and thus probably over-estimate the subsidence that Brittany underwent during the Holocene. This misfit could not be resolved with significant changes to the size and deglaciation histories of the BIIS, suggesting the source of the misfit may be related to (i) errors in the pattern and amounts of meltwater production from the far-field ice sheets, (Antarctic, Iceland, Patagonia and Arctic sea) which are predominately driving the RSL rise across the study region and to (ii) lateral variations in the Earth's structure across the English Channel, especially in the upper-mantle viscosity, which occur over relatively short-scale lateral distances and (iii) potential misfits in the adopted FIS history. More generally, this work highlights the importance for future work to consider the potential role played by such lateral heterogeneities in the RSL signal across this region. Generally, this work again identifies the importance of developing three-dimensional earth models and of further considering the potential roles played by tectonic features in isostatic adjustment dynamics.

Several questions, pertaining to the isostatic dynamics at the scale of Northwestern Europe are still to be resolved. Providing reliable answers to these questions will allow a better prediction of future regional RSL variations. Our work emphasizes the need for more new reliable index points along the coasts of Eastern North Atlantic and of the English Channel, in order to estimate more precisely the relative contribution of the hydro- and glacio-isostatic components of the RSL rise, as well as to better constraint three-dimensional lateral and vertical variations in the Earth structure across the English Channel. Such work is already underway. Furthermore, as such distal regions can be shown to the highly sensitive to changes in the far-field eustatic signal, such new data could provide new information for the rates of ESL rise over the Holocene.

The results of this study insist on the fact that GIA models are still unable to provide a reliable evaluation of the subsidence history for the Brittany region. Yet, recent RSL rise rates are calculated from modern tide-gauge records corrected from land-movements by using GIA predictions. Considering the inconsistence of the GIA prediction with the geological RSL records, it is likely that modern RSL rise rates obtained from Brest tide-gauge record are under-evaluated.

Supporting information (Supplementary Online Material)

Commentaire [BVVL16]: ADDED SOME MORE SUPPLEMENTARY ONLINE MATERIAL

Additional supporting information can be found as Supplementary Online Material in the online version of this article:

S1**-** Building of the salt-marsh surface sediments geochemical modern referential and application to Holocene cores

S2- Numerical outputs of the paleo tidal modelling at our study sites.

S3- RSL spatial plots from "BIIS", Glac-1B and ICE-5G (VM2a) GIA model predictions for the 7 ky, 6ky, 5ky and 4ky B.P periods.

Acknowledgment

This work is a contribution to the ANR COCORISCO (French National Research Agency Program for the Assessment and Management of Coastal Risks, ANR 2010-CEPL-001-01, Pôle-Mer Bretagne), task 2 "Historical and geological signatures". Financial support for equipment, fieldwork and analyses was provided by ANR COCORISCO, as well as by the host organizations: Geomer UMR 6654 LETG and Domaines Océaniques UMR 6538. G. Spada is funded by a DiSBeF grant (CUP H31J13000160001). The authors are grateful to N. Guidicelli and C. Kermagoret for their outstanding help in the field. This paper is a contribution to the PALSEA2 program of PAGES IGBP and the INQUA Commission on Coastal and Marine Processes. The authors are very grateful to Roland Gehrels and to one anonymous reviewer whose comments and suggestions significantly helped to push the manuscript further.

References

Allen J.R.L. (2000) - Morphodynamics of Holocene salt marshes: a review sketch from the Atlantic and Southern North Sea coasts of Europe, *Quaternary Science Reviews*, 19, 1155-1231.

Baeteman C., Scott D.B., Van Strydonck, M. (2002) - Changes in coastal zone processes at a high sea-level stand: a late Holocene example from Belgium, *Journal of Quaternary Science*, 17, 5-6, 547-559.

Ballantyne, C. K. 2010a: Extent and deglacial chronology of the last British-Irish Ice Sheet: implications of exposure dating using cosmogenic isotopes, *Journal of Quaternary Science 25*, 515–534.

Ballantyne, C. K., Stone, J. O. & McCarroll, D. 2008: Dimensions and chronology of the last ice sheet in western Ireland, *Quaternary Science Reviews 27*, 185–200.

Ballantyne, C. K. & Stone J. O.: Trimlines, blockfields and the vertical extent of the last ice sheet in southern Ireland, *Boreas*. 10.1111/bor.12109. ISSN 0300-9483.

Behre K.E. (1986) - Analysis of botanical macro-remains. In: Sea-level Research: A manual for the collection and evaluation of data (Van de Plassche ed.), Geobooks, Norwich, pp. 413-433

Bradley S.L. (2011) - Using Sea-level and Land Motion Data to Develop an Improved Glacial Isostatic Adjustment Model for the British Isles. PhD thesis, Durham University, 260 p.

Bradley S.L., Milne G.A., Teferle F.N., Bingley R.M. and E.J. Orliac (2009) – Glacial isostatic adjustment of the British Isles: new constraints from GPS measurements of crustal motion, *Geophysical Journal International*, 178, 14-22.

Bradley S.,L**,** Milne G., A, Horton B. and Zong Y. (2015, *submitted*). Modelling sea level data from China and Malay-Thailand Peninsula to estimate Holocene ice-volume equivalent sea level.

Bradley S., Milne G.A., Shennan I., Edwards R. (2011) - An improved Glacial Isostatic Adjustment model for the British Isles, *Journal of Quaternary Science* 26, 5, 541-552.

Brain M.J., Long A.J., Petley D.N., Horton B.P., Allison R.J. (2011) - Compression behaviour of minerogenic low energy intertidal sediments, *Sedimentary Geology.* 233, 28-41.

Brain M.J., Long A.J., Woodroffe S.A, Petley D.N., Milledge D.G., Parnell A.C. (2012) - Modelling the effects of sediment compaction on salt marsh reconstruction of recent sea-level rise, *Earth and Planetary Science*, 346-348, 180-193.

Brain M.J., Kemp A.C., Horton B.P., Culver S.J., Parnell A. C., Cahill N. (2015) - Quantifying the contribution of sediment compaction to late Holocene salt-marsh sea-level reconstructions, North Carolina, USA, *Quaternary Research*, 83, 1, 41-51.

Briggs R., Pollard D., Tarasov L. (2014) - A data constrained large ensemble analysis of Antarctic evolution since the Eemian, *Quaternary Science Reviews*, 103, 91-115.

Clark C. D., Hughes A. L.C., Greenwood S. L., Jordan C., Sejrup H.P. (2012) - Patter and timing of retreat of the last British-Irish Ice Sheet, *Quaternary Science Reviews*, 44, 112-146.

Clark P. U., Tarasov L. (2014) - Closing the sea level budget at the Last Glacial Maximum, *PNAS,* 111, 45, 15861-15862.

Clarke M. L., Rendell H. M. (2009) - The impact of North Atlantic storminess on western European coasts: A review, *Quaternary International*, 195, 31-41.

Cleveringa J. (2000) - Reconstruction and modelling of Holocene coastal evolution of the western Netherlands. PhD thesis, Utrecht, 1-198.

Delibrias G. & Guillier M.T. (1971) - The sea level on the Atlantic coast and the Channel for the last 10,000 years by the ^{14}C method, *Quaternaria*, 14, 131-135.

Dellwig O., Böttcher M.E., Lipinski M., Brumsack H.-J. (2002) - Trace metals in Holocene coastal peats and their relation to pyrite formation (NW Germany), *Chemical Geology*, 182, 423-442.

Dellwig O., Watermann F., Brumsack H.-J., Gerdes G., Krumbein W.E. (2001) - Sulphur and iron geochemistry of Holocene coastal peats (NW Germany): a tool for paleoenvironmental reconstruction, *Palaeogeography, Palaeoclimatology, Palaeoecology*, 167, 359-379.14.

Douglas B. C. (2001) - Sea level change in the era of the recording tide gauge, in Sea Level Rise: History and Consequences, Int. Geophys. Ser., vol. 75, edited by B. Douglas, M. Kearney, and S. Leatherman, chap. 3, pp. 37–64, Academic, San Diego, Calif.

Douglas B. C. (2008) - Concerning evidence for fingerprints of glacial melting, *Journal of Coastal Research*, 24, 218–227.

Crastes de Paulet F. (2013) – Utilisation des cartes piézométriques de Wallonie dans le cadre de l'étude des nappes transfrontalières (France-Belgique), Colloque 'La carte hydrogéologique de Wallonie : un outil au service de tous', Jambes (namur) –Belgique, 16 mai 2013.

Engelhart S.E., Horton B.P. (2012) - Holocene sea level database for the Atlantic coast of the United States, *Quaternary Science Reviews*, 54, 12-25.

Engelhart S., Horton B.P., Vane C.H., Nelson A.R., Witter R.C., Brody S.R, Hawkes A.D. (2013) - Modern foraminifera, δ^{13}C, and bulk geochemistry of central Oregon tidal marshes and their application in paleoseismology*, Palaeogeography, Palaeoclimatology, Palaeoecology 377, 13-2.*

Enio M.S.K., Shamshuddin J., Fauziah C.I. , Husni M.H.A (2011) - Pyritization of the Coastal Sediments in the Kelantan Plains in the Malay Peninsula during the Holocene, *American Journal of Agricultural and Biological Sciences*, 6, 3, 393-402.

Farrel W.E., Clark J.A. (1976) - On postglacial Sea level, *Geophysical Journal of the Royal Astronomical Society*, 46, 3, 647-667.

Fernane A., Gandouin E., Penaud A., Van Vliet-Lanoë B., **Goslin J.**, Vidal M., Delacourt C. (2014) - Coastal paleoenvironmental record of the last 7 ka BP in NW France: infra-millenar climatic and anthropic Holocene signals, *The Holocene*, doi: 10.1177/0959683614551223

Gandouin E. (2003) - Enregistrement paléoclimatique de la transgression Holocène ; signature paléoenvironnementale des *Chironomidae* (Diptères) du bassin de Saint-Omer (France). Thèse de Doctorat en Sciences de la Terre, USTL, 256 pp.

Gehrels W.R. (1999) - Middle and late Holocene sea-level changes in eastern Maine reconstructed from foraminiferal saltmarsh stratigraphy and AMS ^{14}C dates on basal peats. *Journal of Quaternary Research* 52, 350-359.

Gehrels W.R., Belknap D.F., Pearce B.R., Gong B. (1995) - Modeling the contribution of M2 tidal amplification to the Holocene rise of mean high water in the Gulf of Maine and the Bay of Fundy. *Marine Geology* 124, 71-85.

Gehrels W.R., Anderson W.P. (2014) - Reconstructing Holocene sea-level change from coastal freshwater peat: A combined empirical and model-based approach, *Marine Geology*, 353, 140-152.

Gehrels W.R., Belknap D.F., Kelley J.T. (1996) - Integrated high-precision analyses of Holocene relative sea-level changes: Lessons from the coast of Maine. *Geological Society of America Bull*etin 108, 9, 1073-1088.

Gehrels, W.R., 2010a. Late Holocene relative sea-level changes and crustal motion around the British Isles: implications for future sea-level predictions. *Quaternary Science Reviews*, 29, 1648-1660, doi:10.1016/j.quascirev.2009.09.015.

Gehrels, W.R., Dawson, D.A., Shaw, J., Marshall, W.A. (2011) - Using Holocene relative sea-level data to inform future sea-level predictions: an example from Southwest England. *Global and Planetary Change,* 78, 116–126. http://dx.doi.org/10.1016/j.glopacha.2011.05.013.

Goslin J., Van Vliet-Lanoë B., Delacourt C., Fernane A., Gandouin E., Hénaff A., Penaud A., Stephan P., Suanez S. (2013) - Holocene relative sea-level changes in western Brittany (France) between 7600 and 4000 cal. BP: Reconstitution from basal-peat deposits, *Géomorphologie: Relief, Processus, Environnement*. 4, 425-444

Goslin J. (2014) – Holocene Relative Sea-Level reconstruction in the Finistère region (Brittany, France): regional dynamics, local responses, PhD thesis, University of Brest, p 1-355.

Greaves M., Hipkin R., Calvert C., Fane C., Rebischung P, Duquenne F., Harmel A., Coulomb A., Duquenne H. (2008) -Connection of British and French levelling networks - Application to UELN, Proceeding of EUREF Symposiu 2007, London. To be found at: *www.euref.eu*

Healy MG. 1993. Coastal evolution and relative sea-level change in west Cornwall, UK. PhD thesis, National University of Ireland, University College Cork.

Healy MG. 1995. The lithostratigraphy and biostratigraphy of a Holocene coastal sediment sequence in Marazion Marsh, west Cornwall, UK with reference to relative sea-level movements. Marine Geology 124: 237–252.

Hijma M.P., Cohen K.M. (2010) - Timing and magnitude of the sea-level jump preluding the 8200 yr event, *Geology*, 38, 3, 275-278.

Hijma M.P., Cohen K.M. (2011) - Holocene transgression of the Rhine river mouth area, The Netherlands/Southern North Sea: palaeogeography and sequence stratigraphy, *Sedimentology*, 58, 6, 1453-1485.

Horton B.P., Edwards R.J., Lloyd J.M. (2000) - Implications of a microfossil transfer function in Holocene sea-level studies, *Geological society special publication*, 166, 41-54

Horton B.P., Corbet R., Culver S.J., Edwards R.J., Hillier C. (2006) - Modern saltmarsh diatom distributions of the Outer Banks, North Carolina, and the development of a transfer function for high resolution reconstructions of sea level*, Estuarine, Coastal and Shelf Science*, 69, 381-394.

Horton B., Shennan I. (2009) - Compaction of Holocene strata and the implications for relative sea level change on the east coast of England, *Geology,* 37, 12, 1083-1086.

Jelgersma S. (1961) - Holocene sea-level changes in The Netherlands, *Mededelingen van de Geologische Stichting*, serie C VI 7, 1-100.

Kemp A.C., Horton B.P., Reide Corbet R., Culver S.J., Edwards R.J., Van de Plassche O. (2009) - The relative utility of foraminifera and diatoms for reconstructing late Holocene sea-level change in North Carolina, USA, *Quaternary Research*, 71, 9-21.

Kemp A.C., Telford R.J., Horton B.P., Anisfeld S.C., Sommerfield C.K. (2013) - Reconstructing Holocene sea level using salt-marsh foraminifera and transfer functions: lessons from New Jersey, USA, *Journal of Quaternary Science*, 28, 6, 617-629

Kiden P. (1995) - Holocene relative sea-level change and crustal movement in the southwestern Netherlands. Marine Geology, 124, 21-41.

Kiden P., Denys L., Johnston P. (2002) - Late Quaternary sea-level change and isostatic and tectonic land movements along the Belgian–Dutch North Sea coast: geological data and model results, *Journal of Quaternary Science*, 17, 5-6, 535-546.

Kuchar J., Milne G., Hubbard A., Patton H., Bradley S., Shennan I., Edwards R. (2012) – Evaluation of a numerical model of the British-Irish ice sheet using relative sea-level data: implications for the interpretation of trimline observations, *Journal of Quaternary science*, 27, 2, 597-605.

Lambeck K. (1997) - Sea-level change along the French Atlantic and Channel coasts since the time of the Last Glacial Maximum, *Palaeogeography, Palaeoclimatology, Palaeoecolecology* 129, 1-2, 1-22.

Leorri E., Cearreta A., Milne G. (2012) - Field observations and modeling of Holocene sea-level changes in the southern Bay of Biscay: implications for understanding current rates of relative sea-level change and vertical land motion along the Atlantic coast of SW Europe, *Quaternary Science Reviews* 42, 59-73.

Long A.J., Waller M.P., Stupples P. (2006) - Driving mechanisms of coastal change: Peat compaction and the destruction of late Holocene coastal wetlands. *Marine Geology* 225, 63-84.

Massey A.C., Paul M.A., Gehrels W.R., Charman DJ. (2006b) - Autocompaction in Holocene coastal back-barrier sediments from south Devon, southwest England, UK. *Marine Geology* 226, 3-4, 225-241.

Massey A.C., Gehrels W.R., Charman D.J., Milne G.A., Peltier W.R., Lambeck K., Selby K.A. (2008) – Relative sea-level change and postglacial adjustment along the coast of south Devon, UK. *Journal of Quaternary Science* 23, 5, 415-433.

Mauquoy D., van Geel B., 2007. Mire and peat macros. In: Encyclopedia of Quaternary Science, Volume 3 (S.A. Elias, editor) p. 2315-2336, Elsevier.

Milne G.A., Peros M. (2013) - Data–model comparison of Holocene sea-level change in the circum-Caribbean region, *Global and Planetary Change*, 107, 119-131.

Mitrovica J.X., Milne G.A. (2002) - On the origin of ocean siphoning, *Quaternary Science Reviews*, 21, 2179-2190.

Mitrovica J.X., Milne G.A. (2003) - On post-glacial sea level: i. General theory, *Geophys. J. Int.*, 153, 253-267.

Mitrovica J.X., Peltier W.R. (1991) - On postglacial geoid subsidence over the equatorial oceans, *Journal of Geophysical Research*, 96, 20053– 20071.

Morzadec-Kerfourn M.-T. (1974) - *Variation de la ligne de rivage armoricaine au Quaternaire. Analyses polliniques de dépôts organiques littoraux*. Ph.D thesis, University of Rennes 1, 208 p.

Neill S.P., Scourse J.D., Uheara K. (2010) - Evolution of bed shear stress distribution over the northwest European shelf seas during the last 12,000 years, *Ocean Dynamics,* 60, 1139-1156.

Nordman M., Milne G., Tarasov L. (2015) – Reappraisal of the Angerman River decay time estimate and it application to determine uncertainty in Earth viscosity structure, *Geophysical Journal International*, 201, 811-822.

Peltier W.R. (2001) - Global glacial isostatic adjustmentand modern instrumental records ofrelative sea level history. pp. 65-95 in *Sea Level Rise: History and Consequences*. B.C. Douglas,M.S. Kearney, and S.P. Leatherman, eds, International Geophysics Series, vol. 75. Academic Press.

Peltier W.R. (2004) -. Global Glacial Isostasy and the Surface of the Ice-Age Earth:The ICE-5G (VM2) Model and GRACE*, Annual Review of Earth and Planetary Science, 32,111-149.*

Peltier W.R., Fairbanks R.G. (2006) - Global glacial ice volume and Last Glacial Maximum duration from an extended Barbados sea level record. *Quaternary Science Reviews*, 25, 3322-3337.

Picado A., Lopes C.L., Mendes R., Vaz N., Dias J.M. (2013) - Storm surge impact in the hydrodynamics of a tidal lagoon: the case of Ria de Aviero, *In:* Conley D.C., Masselink G., Russell P.E. and O'Hare T.J. (eds.), *Proceedings 12th International Coastal Symposium* (Plymouth, England), *Journal of Coastal Research*, Special Issue No. 65, 796-801, ISSN 0749-0208

Rebischung P., Duquenne H., duquenne F. (2009) - The new French zero-order levelling network – First global results and possible consequences for UELN, *Proceedings of EUREF 2008 Symposium*, *Brussels,* 2009*.*

Reimer P. J., Bard E., Bayliss A., Beck J. W., Blackwell P. J.,Ramsey C. B., Buck C. E., Cheng H., Edwards R. L., Friedrich M., Grootes P. M., Guilderson T. P., Haflidason H., Hajdas I.,Hatte C., Heaton T. J., Hoffmann D. L., Hogg A. G., Hughen K. A., Kaiser K. F., Kromer B., Manning S. W., Niu, M., Reimer R. W., Richards D. A., Scott E. M., Southon J. R., Staff R. A., Turney C. S. M. & Van Der Plicht J. (2013) - Intcal13 and Marine13 radiocarbon age calibration curves 0-50,000 years cal BP. *Radiocarbon, 55*, 1869–1887.

Root B.C., Tarasov L., Van der Wal W. (2015) - GRACE gravity observations constrain Weichselian ice thickness in the Barents Sea, Geophysical Research Letters, doi: 10.1002/2015GL063769.

Shennan I., Horton B. (2002) - Holocene land- and sea-level changes in Great Britain, *Journal of Quaternary Science,* 17, 5-6, 511-526.

Shennan I., Lambeck K., Flather R., Horton B., McArthur J., Innes J., Lloyd J., Rutherford M., Wingfield R. (2000) – Modelling western North Sea palaeogeographies and tidal changes during the Holocene, *Geological Society, London, Special Publications 2000,* 166, p. 299-319, doi: 10.1144/GSL.SP.2000.166.01.15

Shennan I., Bradley S., Milne G., Brooks A., Bassett S., Hamilton S. (2006) - Relative sea-level changes, glacial isostatic modelling and ice-sheet reconstructions from the British Isles since the Last Glacial Maximum, *Journal of Quaternary Science*, 21, 6, 585-599.

Shennan I., Milne G., Bradley S. (2012) - Late Holocene vertical land motion and relative sea-level changes: lessons from the British Isles, *Journal of Quaternary Science,* 27, 1, 64-70.

Shennan I., Long A., Horton B.P. (2015) – Handbook of sea-level research, Wiley, 600 p., ISBN: 978-1-118-45258-5.

SHOM 2013: *Marine Altimetric References, Cotes du zero hydrographique et niveaux caractéristiques de la marée*. Edition SHOM, Brest. 113 pp.

Spada G., Melini D., Galassei G, Colleoni F. (2012) - Modeling sea-level changes and geodetic variations by glacial isostasy: the improved SELEN code, arXiv:1212.5061v1.

Stéphan P. and Goslin J. (*2014*) -Evolution du niveau marin relatif à l'Holocene le long des côtes françaises de l'Atlantique et de la Manche : réactualisation des données par la méthode des « sea-level index points », *Quaternaire, 25, 4, 295-312.*

Stephan P., Goslin J., Pailler Y., Manceau R., Van Vliet-Lanoë B., Hénaff A;, Delacourt C. (2015) - Holocene salt-marsh sedimentary infillings and relative sea-level changes in West Brittany (France) based on foraminifera transfer functions, *Boreas*, 44, pp. 153–177. DOI:10.1111/bor.12092.

Tamisiea M.E., Mitrovica. J.X. (2011) - The moving boundaries of sea level change:Understanding the origins of geographic variability. *Oceanography* 24(2):24–39, doi:10.5670/oceanog.2011.25.

Tarasov L., Peltier W.R. (2002) - Greenland glacial history and local geodynamic consequences, *Geophysical Journal International*, 150, 198-229.

Tarasov L., Dyke A.S., Neal R.M., Peltier W.R. (2012) - A data-calibrated distribution of deglacial chronologies for the North American ice complex from glaciological modeling, *Earth and Planetary Science letters*, 315-316, 30-40.

Tarasov L. (2013) - GLAC-1b: a new data-constrained global deglacial ice sheet reconstruction from glaciological modelling and the challenge of missing ice. *Geophys. Res. Abstr*. 2013, 15, EGU2013-12342.

Ters M. (1973) - Les variations du niveau marin depuis 10000 ans le long du littoral atlantique français. *In Le Quaternaire, géodynamique, stratigraphie et environnement*. CNRS, Paris, 114-135.

Ters M. (1986) - Variations in Holocene sea level on the French Atlantic coast and their climatic significance. *In* Rampino M.R., Sanders J.E, Newman W.S, Königsson L.K. (Eds.): *Climate: History, Periodicity and Predictability*. Van Nostrand Reinhold, New York, 204-237.

Tooley M. J. (1982) - Sea-level changes in northern England. *Proceedings of the Geologist's Association*, 93, 43-51.

Törnqvist T.E., Van Ree M.H.M., Van't Veer R., VanGeel B. (1998) - Improving methodology for high-resolution reconstruction of sea-level rise and neotectonics by paleoecological analysis and AMS ^{14}C dating of basal peats. *Quaternary Research,* 49, 1, 72-85.

Törnqvist T.E., Gonzales J.L., Newsom L.A., Van der Borg K., De Jong A.F.M., Kurnik C.W. (2004b) - Deciphering Holocene sea-level history on the U.S. Gulf Coast: A high-resolution record from the Mississippi Delta. *Geological Society of America Bull*etin 116, 7-8, 1026-1039.

Tushingham M.A. et Peltier W.R. (1991) - ICE-3G A new global model of late Pleistocene deglaciation based on geophysical predictions of post-glacial relative sea-level change, *Journal of Geophysical Research,* 96 : 4497-4523.

Uheara K., Scourse J.D., Horsburgh K.J., Lambeck K., Purcell A.P. (2006) - Tidal evolution of the northwest European shelf seas from the Last Glacial Maximum to the present. *Journal of Geophysical Research,* 11, Issue C9.

Van Asselen S., Stouthamer E., Van Asch T.W.J. (2009) – Effects of peat compaction on delta evolution: A review on processes, responses, measuring and modeling, *Earth Science Reviews*, 92, 35-51.

Van de Plassche O. (1991) - Coastal submergence of the Netherlands, NW Brittany (France), Delmarva Peninsula (VA, USA) and Connecticut (USA) during the last 5500 to 7500 sidereal years. *In* Sabadini R. (Ed.): *Glacial Isostasy, Sea Level and Mantle Rheology*. Kluwer, Dordrecht, 285-300.

Van Geel B., Buurman J., Waterbolk H.T. (1996) - Archeological and paleoecological indications for an abrupt climate change in The Netherlands and evidence for climatological teleconnections around 2650 BP. *Journal of Quaternary Science* 11, 451-460.

Van Vliet-Lanoë B., Goslin J., Hallegouët B., Hénaff A., Delacourt C., Fernane A., Franzetti M., Le Cornec E., Le Roy P., Penaud A. (2014a) –Middle to late Holocene storminess in Brittany (NW France). Part I: Morphological impact and stratigraphical record, *The Holocene*, 24, 4, 413–433.

Van Vliet-Lanoë B., Penaud A., Hénaff A., Delacourt C., Fernane A., Goslin J., Hallégouët B., Le Cornec E. (2014b) -Middle to late Holocene storminess in Brittany (NW France). Part II: The chronology of events and climate forcing, *The Holocene*, 24, 4, 434-453

Vink A., Steffen H., Reinhardt L., Kaufmann G. (2007) - Holocene relative sea-level change, isostatic subsidence and the radial viscosity structure of the mantle of northwest Europe (Belgium, theNetherlands, Germany, southern North Sea). *Quaternary Science Reviews* 26, 3249-3275.

Wang Y., Frank Bohlen W., O'Donnell J. (2000) - Storm enhanced bottom shear stress and associated sediment Entrainment in a moderate energetic estuary, *Journal of Oceanography*, 56, 311-317.

Watts, A. B. (2001) - *Isostasy and Flexure of the Lithosphere*, Cambridge, Univ. Press, New York.

Whitehouse P., Latychev C., Milne A., Mitrovica J. X., Kendall R. (2006) - Impact of 3-D Earth structure on Fennoscandian glacial isostatic adjustment: Implications for space-geodetic estimates of present-day crustal deformations, *Geophysical Research letters*, 33, L13502.

Woodworth P. L. (1987) - Trends in U. K. mean sea level, *Marine Geodesy*, 11,57– 87.

Woodworth P., Shaw S., Blackman D. (1991) - Secular trends in mean tidal range around the British Isles and along the adjacent European coastline, *Geophysical Journal International*,104, 3, 593-609.

Wöppelmann G., Marcos M. (2012)- Coastal sea level rise in southern Europe and the nonclimate contribution of vertical land motion, *Journal of Geophysical Research*, 117, C01007, doi:10.1029/2011JC007469.

Wöppelmann G., Pouvreau N., Coulomb A., Simon B., P. L. Woodworth P.L. *(*2008*),* Tide gauge datum continuity at Brest since 1711: France's longest sea-level record*, Geophysical Research Letters,* 35*, L22605, doi.*

Wu P., Ni Z. , Kaufmann G. (1998) - Postglacial Rebound with Lateral Heterogeneities : from 2D to 3D modeling.in "Dynamics of the Ice Age Earth: A Modern Perspective" edited by P.Wu, Trans Tech Publ., Switzerland, p.557-582.

Zhu H., Bozdag E., Peter D., Tromp J. (2012) – Structure of the European upper-mantle revealed by adjoint topography, *Nature geoscience*, DOI:10.1038/NGEO1501

Site	Reference tide-gauge(s) location	Spring Tidal range	HAT (m NGF)	MHWST (m NGF)	MHWNT (m NGF)	MTL (m NGF)	MLWNT (m NGF)	MLWST (m NGF)	LAT (m NGF)
Guissény	Brignogan / Aber Wrac'h	7.52	4.74	4.06	2.36	0.62	-1.07	-3.46	-4.37
Landéda	Aber Wrac'h	7.52	4.45	3.73	2.08	0.39	-1.17	-3	-3.95
Porsmilin	Le Trez-Hir	5.55	4	3.17	1.67	0.39	-0.93	-2.38	-3.21
Treffiagat	Le Guilvinec	4.2	3.16	2.66	1.56	0.50	-0.44	-1.54	-2.38
Kermor-Tudy	Loctudy	4.20	3.09	2.45	1.35	0.41	-0.65	-1.75	-2.40
Guidel	Le Pouldu	4.15	2.78	2.23	1.18	0.17	-0.82	-1.92	-2.65

Table 1 - Present-day tidal levels on the studied sites (from SHOM, 2013). Levels are given related to the French ordnance datum (m NGF)**.** HAT (Highest Astronomical Tide), MHWST (Mean High Water Spring Tides), MHWNT (Mean High Water Neap Tides), MTL (Mean Tide Level), MLWNT (Mean Low Water Neap Tides) MLWST (Mean Low Water Spring Tides), LAT (Lowest Astronomical Tide)

Source of vertical uncertainties	Amplitude
Coring process	Hand-auguring : - 0.02m / meter depth Percussion-coring: null Screw-drilling: ± 0.5 m
Levelling	DGPS measurement : ± 0.02m Geodetic benchmark accuracy : ± 0.1 m
Sampling	± 0.02 m
Tidal levels	± 0.05 m when estimated from distant stations

Table 2 - Errors terms used in RSL reconstruction.

Deposit environment	$\delta^{13}C$ (‰)	TOC (%)	TN (%)	Pollen	Plant macro-remains	Foraminifera (if present)	Pyrite	Indicative meaning
Biozone 2	-28 / -26.4	1 - 8	0.1 - 0.85	Presence of halophilous species	E.g. Halimione sp., Triglochin sp., Limonium vulgare	Mid to low marsh species	Embedded within the sedimentary matrix	(SWLI 179 – SWLI 129) /2
Biozone 3	-28 / - 25.5	>4.95	>0.9	Presence of halophilous species	E.g. Juncus maritimus, Scirpus maritimus, Halimione portulacoides	high marsh species	Embedded within the sedimentary matrix	(SWLI 212 – SWLI 183) /2
Undifferentiatd brackish peat deposit	n/a	n/a	n/a	Presence of halophilous species	E.g. Phragmites australis, Juncus roemerianus, Juncus maritimus	Present	Embedded within the sedimentary matrix	(HAT – MHWNT) /2
Freshwater peat deposit	n/a	n/a	n/a	Absence of halophilous species	Freshwater reed species	absent	absent	High limiting (> MHWST)

1247 **Table 3 – Indicative meanings used to reconstruct RSL from foraminifera poor sedimentary sequences.** Reader is invited to refer to Supplementary

1248 Online Material S1 for further explanations on the building of the modern geochemical reference.

Index n°	Core	14C Lab code	Age B.P. conv.	Cal. a BP (2σ)	Elevation		Position	$\delta^{13}C$	TOC	TON	C/N	Indicative meaning (m)	Vertical uncertainties (m)						RSL (m relative to present-day MHWST))	RSL corrected for regional changes in paleo tidal ranges	
				min (med. Prob.) max	(m NGF)	Relative to local HWST		‰	%	%			Indicative range	Coring	Sampling	Levelling	Distant tidal station	Total		RSL position (m relative to present-day MHWST)	Indicative range (m)
1	GUIS-C2	UBA-15681	431 ± 28	527 (500) 338	3.2	-0.8	I	-27.63	4.35	0.33	13.09	-1.65	0.94	0	0.02	0.12	0.05	0.94	0.85 ± 0.94	0	0
2	GL2	Poz-48807	970 ± 30	933 (860) 796	1	-1.226	I	-26.40	4.74	0.36	13.30	-0.99	0.56	0.5	0.02	0.12	0.05	0.76	-0.23 ± 0.76	-0.04	0
3	KIX-1	SacA-23976	2305 ± 30	2084 (1964) 1864	0.8	-1.65	I	-19.95	1.17	0.11	11.09	-0.98	0.56	0.5	0.02	0.12	0	0.76	-0.67 ± 0.76	-0.07	0
4	KIX-3	SacA-23978	2875 ± 30	2774 (2703) 2565	-1.4	-3.85	I	-22.40	3.03	0.28	10.70	-0.98	0.56	0.5	0.02	0.12	0	0.76	-2.87±0.76 (*)	n/d	n/d
5	GUIS-C2	UBA-15685	2 666 ± 25	2844 (2770) 2746	0.05	-3.63	I	-27.76	2.35	0.18	12.86	-1.65	0.94	0	0.02	0.12	0.05	0.95	-1.98 ± 0.94	-0.20	0.02
6	KX1	Poz-42852	3425 ± 35	3825 (3676) 3581	-1	-3.45	I	-20.82	5.60	0.46	12.27	-0.98	0.56	0.5	0.02	0.12	0	0.76	-2.47 ± 0.76	-0.12	0
7	GUIS-C2	Poz-49796	4165+/-35	4830 (4709) 4580	-0.8	-4.48	I	-28.01	36.92	1.50	24.60	-0.07	0.48	0	0.02	0.12	0.05	0.50	-4.41 ± 0.50	-0.19	0.02
8	TREF	Poz-45390	4340 ± 40	5035 (4913) 4839	-0.95	-3.61	BB	-25.27	5.56	0.44	12.66	-1.035	0.59	0.09	0.02	0.12	0.05	0.61	-2.58 ± 0.61	-0.28	0.01
9	GL1	Poz-49806	4395 ± 35	5212 (4957) 4859	-2	-4.226	I	-25.24	0.20	0.02	10.24	-0.99	0.56	0.5	0.02	0.12	0.05	0.76	-3.23 ± 0.76	-0.26	0.04
10	KX-3	Poz-36731	4530 ± 30	5309 (5156) 5053	-2.2	-4.65	I	-23.67	12.15	0.64	19.02	-0.98	0.56	0.5	0.02	0.12	0	0.76	-3.67±0.61	-0.17	0
11	GUIS-C2	Poz-49798	4530+/-35	5311 (5159) 5050	-0.95	-4.63	I	-27.90	16.89	1.04	16.22	-0.07	0.48	0	0.02	0.12	0.05	0.50	-4.56 ± 0.5	-0.20	0.02
12	KX-2	Poz-42853	4480 ± 35	5292 (5167) 4978	-1.8	-4.25	I	-22.07	3.60	0.32	11.38	-0.98	0.56	0.5	0.02	0.12	0	0.76	-3.27± 0.61	-0.17	0
13	KX-4	Poz-42854	4800 ± 40	5606 (5520) 5334	-2.49	-4.94	I	-26.62	23.51	1.21	19.51	-0.04	0.3	0.5	0.02	0.12	0	0.60	-4.9 ± 0.60	-0.19	0
14	PM1	Poz-42858	5000 ± 35	5891 (5728) 5645	-1.5	-4.67	I	-28.61	23.92	1.26	19.00	-0.1	0.4	0	0.02	0.12	0.05	0.42	-4.57 ± 0.42	0.09	0
15	KIX-4	Poz-42850	5215 ± 35	6129 (5965) 5908	-1.8	-4.25	BB	-21.96	0.28	0.04	8.07	-0.98	0.56	0.5	0.02	0.12	0	0.76	-3.27±0.76	-0.21	0
16	PM1	Poz-42860	5365 ± 35	6277 (6170) 6006	-2.27	-5.44	I	-28.00	13.56	0.65	20.82	-1.3	0.76	0	0.02	0.12	0.05	0.77	-4.1 ± 0.77	0.10	-0.01
17	GUIS-C2	UBA-15686	5 563 ± 31	6403 (6351) 6299	-1.52	-5.2	BB	-27.52	9.66	0.64	15.13	-0.07	0.48	0	0.02	0.12	0.05	0.50	-5.13 ± 0.5	-0.13	0.02
18	GL2	Poz-48773	5910 ± 40	6846 (6730) 6651	-5.59	-7.816	I	-24.59	1.16	0.10	11.25	-0.99	0.56	0.5	0.02	0.12	0.05	0.76	-6.81 ± 0.76	-0.13	0
19	KIX-5	Poz-42851	5990 ± 40	6939 (6829) 6736	-4.6	-7.05	B	-22.31	3.22	0.21	15.51	-0.98	0.56	0.5	0.02	0.12	0	0.76	-6.07 ± 0.76	n/a	n/a
20	TAR-S2	UBA-15458	6 001 ± 28	6927 (6845) 6750	-3.6	-7.38	BB	-26.9	-	-	-	-0.44	1.21	0.06	0.02	0.12	0.05	1.22	-6.95 ± 1.22	0.13	0.03
21	PM1	Poz-42861	6150 ± 40	7164 (7060) 6943	-3.3	-6.47	BB / HL	-	-	-	-	-	-	-	-	-	-	-	< - 6.47	n/a	n/a
22	GUIS-S2	UBA-15460	6 033 ± 29	6951 (6880) 6791	-3.5	-7.18	BB	-	-	-	-	-0.44	1.21	0.02	0.02	0.12	0.05	1.22	-6.74 ± 1.22	0.13	0.03
23	GL1	Poz-47039	6650 ± 40	7587 (7530) 7444	-8	-10.226	B	-26.38	15.51	0.77	20.08	-0.04	0.30	0.5	0.02	0.12	0.05	0.60	-10.18 ± 0.60	-0.04	0
24	GL2	Poz-49808	7090 ± 40	7996 (7923) 7840	-8.39	-10.616	B	-24.84	1.40	0.13	10.61	-0.98	0.56	0.5	0.02	0.12	0.05	0.76	-9.63±0.76	0.05	0

Table 4 - Details of the new Holocene RSL data obtained in this study. (*) indicates rejected dates (see text). The last two columns on the right show the correction applied to raw RSL data for changes in paleo tidal ranges. "I" stands for "intercalated" deposits" (uncorrected for compaction), "B" for "basal" deposits and "BB" for "base-of-basal" deposits, "HL" stands for "High Limiting" indexes.

Index n°	Location	Core	14C Lab code	Age B.P. conv.	Cal. a BP (2σ) min (med. Prob.) max	Position	Type	RSL (m relative to present-day MHWST))	Source	Correction for regional changes in paleo tidal ranges (This study) (m)
25	Bay of Brest	P-C2	Erl-10678	3500±60	3957 (3773) 3615	I	SLIP	−3.49 ± 0.67	Stéphan *et al.* (2014)	0.17
26	Bay of Brest	P-C2	Erl-10679	4280±60	5036 (4852) 4625	I	SLIP	−4.17 ± 0.67	Stéphan *et al.* (2014)	0.21
27	Bay of Brest	P-C2	Erl-10680	4640±60	5581 (5394) 5071	I	SLIP	−5.32 ± 0.67	Stéphan *et al.* (2014)	0.21
28	Bay of Brest	T-C2	Erl-10682	940±56	952 (850) 734	I	SLIP	−0.48 ± 0.67	Stéphan *et al.* (2014)	0.04
29	Bay of Brest	T-C2	Erl-10683	3690±70	4235 (4031) 3843	I	SLIP	−3.35 ± 0.67	Stéphan *et al.* (2014)	0.17
30	Bay of Brest	T-C2	Erl-10686	5450±70	6399 (6242) 6015	I	SLIP	−5.32 ± 0.67	Stéphan *et al.* (2014)	0.25
31	Bay of Brest	A-C10	Erl-11753	1081±56	1174 (999) 916	I	SLIP	−0.61 ± 0.67	Stéphan *et al.* (2014)	0.04
32	Bay of Brest	A-C14	Erl-11749	436±55	546 (483) 316	I	SLIP	−0.30 ± 0.67	Stéphan *et al.* (2014)	0.02
33	Bay of Brest	A-C14	Erl-11750	1686±56	1720 (1597) 1415	I	SLIP	−0.97 ± 0.67	Stéphan *et al.* (2014)	0.06
34	Bay of Brest	A-C14	Erl-11751	2340±54	2691 (2372) 2159	I	SLIP	−2.26 ± 0.67 (*)	Stéphan *et al.* (2014)	0.08
35	Bay of Brest	A-C14	Erl-11752	2716±55	2941 (2822) 2748	B	SLIP	−2.96 ± 0.67 (*)	Stéphan *et al.* (2014)	0.13
36	Tresseny	G-C2	UBA 15681	431±28	527 (500) 338	I	SLIP	−0.28 ± 0.55	Stéphan *et al.* (2014)	-0.02
37	Tresseny	G-C3	UBA 15459	4054±32	4785 (4530) 4426	B	SLIP	−3.75 ±1.35	Stéphan *et al.* (2014)	-0.09
38	Trezien	/	GIF-714	3660 ± 115	4385(3994) 3648	BB / HL	SLIP	<2 ± 0,55	Goslin *et al*. (2013) Morzadec-Kerfourn (1974)	n/a
39	Arg.- Gwen.	/	GIF-816	3970 ± 35	4525 (4453) 4297	BB	HL	-3,61 ± 1,75	Goslin *et al*. (2013) Morzadec-Kerfourn (1974	n/a
40	Plou.-Pors.	/	GIF-711	4120 ± 140	5031 (4605) 4184	BB	SLIP	< -1,86 ± 0,55	Goslin *et al*. (2013) Morzadec-Kerfourn (1974	n/a

Table 5 - Holocene RSL data from previous studies (Morzadec-Kerfourn, 1974; Goslin *et al.*, 2013; Stéphan *et al.*, 2014) incorporated to our dataset. (*) indicates rejected dates (see text). The last column on the right show the correction applied to raw RSL data for changes in regional paleo tidal ranges. "I" stands for "intercalated" deposits" (uncorrected for compaction), "B" for "basal" deposits and "BB" for "base-of-basal" deposits, "HL" stands for "High Limiting" indexes.

<u>Supplementary Online Material 2 (Appendix S2)</u>: Numerical outputs of the paleo tidal modelling at our study sites.

Time \ Site	Guissény		Porsmilin		Bay of Brest		Treffiagat		Kermor-Tudy		Guidel	
	Range (m)	%	Range (m)	%	Range (m)	%	Range (m)	%	Range (m)	%	Range (m)	%
NEAP TIDAL RANGES												
0 (control)	3,50	100	2,6	100,0	2,79	100,0	2	100	2	100	2	100
1 Ky B.P	3,50	100	2,59	99,6	2,74	98,2	2	100	2	100	2	100
2 Ky B.P	3,50	100	2,57	98,8	2,69	96,4	2	100	2	100	2,01	100,5
3 Ky B.P	3,50	100	2,56	98,5	2,64	94,6	2,01	100,5	2	100	2,01	100,5
4 Ky B.P	3,50	100	2,55	98,1	2,6	93,2	2,01	100,5	1,99	99,5	2,01	100,5
5 Ky B.P	3,50	100	2,53	97,3	2,55	91,4	2,01	100,5	1,99	99,5	2,02	101
6 Ky B.P	3,50	100	2,52	96,9	2,5	89,6	2,01	100,5	1,99	99,5	2,02	101
7 Ky B.P	3,16	90,3	no data	no data	no data	no data	1,77	88,36	no data	no data	1,78	89
8 Ky B.P	2,82	80,6	no data	no data	no data	no data	1,52	76,02	no data	no data	1,54	77
SPRING TIDAL RANGES												
0 (control)	6,97	100	5,55	100	5,9	100	4,15	100	4,2	100	4,15	100
1 Ky B.P	7,01	100,6	5,53	99,6	5,82	98,6	4,2	101,2	4,23	100,7	4,2	101,2
2 Ky B.P	7,05	101,1	5,52	99,5	5,74	97,3	4,24	102,2	4,27	101,7	4,26	102,7
3 Ky B.P	7,09	101,7	5,5	99,1	5,65	95,8	4,29	103,4	4,3	102,4	4,31	103,9
4 Ky B.P	7,13	102,3	5,48	98,7	5,57	94,4	4,34	104,6	4,34	103,3	4,36	105,1
5 Ky B.P	7,17	102,9	5,46	98,4	5,49	93,1	4,39	105,8	4,37	104,0	4,41	106,3
6 Ky B.P	7,21	103,4	5,45	98,2	5,41	91,7	4,43	106,7	4,41	105,0	4,47	107,7
7 Ky B.P	6,84	98,1	no data	no data	no data	no data	4,22	101,7	no data	no data	4,28	103,1
8 Ky B.P	6,48	93,0	no data	no data	no data	no data	4,01	96,6	no data	no data	4,1	98,8
MAX ANNUAL TIDAL RANGES												
0 (control)	8,73	100	7,2	100	7,68	100	5,54	100	5,49	100	5,43	100,0
1 Ky B.P	8,73	100	7,19	99,9	7,63	99,3	5,54	100	5,49	100	5,43	100,0
2 Ky B.P	8,64	98,9	7,17	99,6	7,58	98,7	5,54	100	5,49	100	5,44	100,2
3 Ky B.P	8,54	97,8	7,16	99,4	7,53	98,0	5,55	100,2	5,49	100	5,44	100,2
4 Ky B.P	8,45	96,7	7,15	99,3	7,49	97,5	5,55	100,2	5,48	99,82	5,44	100,2
5 Ky B.P	8,35	95,6	7,13	99,0	7,44	96,9	5,55	100,2	5,48	99,82	5,45	100,4
6 Ky B.P	8,26	94,6	6,57	91,3	6,53	85,0	5,43	98,0	5,41	98,54	5,49	101,1
7 Ky B.P	8,16	93,5	no data	no data	no data	no data	5,22	94,2	no data	no data	5,31	97,8
8 Ky B.P	7,77	89,0	no data	no data	no data	no data	5,01	90,4	no data	no data	5,13	94,5